

# POLITECNICO DI TORINO

Master's Degree in Communications Engineering



Master's Degree Thesis

## Fundamental Limits of Integrated Sensing and Communication without Perfect Channel State Information

Supervisors

Prof. Giorgio TARICCO

Prof. Natasha DEVROYE

Prof. Daniela TUNINETTI

Prof. Besma SMIDA

Candidate

Simone DI BARI

July 2024

# Summary

This thesis explores the theoretical underpinnings and practical implications of Integrated Sensing and Communication (ISAC) within future wireless networks. As a transformative technology, ISAC merges sensing and communication functionalities to optimize the utilization of spectrum and hardware resources, a necessity driven by the increasing demands of modern applications such as autonomous vehicles and immersive technologies.

The research addresses the critical need to understand the fundamental trade-offs between sensing and communication within ISAC systems. It investigates the Bayesian Cramér-Rao Bound (BCRB) as a metric for evaluating the performance limits of ISAC systems under various conditions. This bound is particularly relevant given the non-realistic nature of assuming known state information in dynamic channel environments, necessitating continuous estimation.

This thesis evaluates the performance of different transmission strategies by developing a comprehensive theoretical model. It balances the conflicting requirements of sensing and communication, thus providing insights into the optimal allocation of power and resources. The simulation results validate the theoretical predictions, demonstrating how ISAC can enhance spectral, energy, and economic efficiencies in next-generation wireless networks.

The findings contribute significantly to the field by laying the groundwork for future research to integrate further and optimize sensing and communication. The methodologies and insights presented in this work are expected to drive the development of advanced ISAC solutions, pushing the boundaries of what is achievable in wireless communication systems.

# Acknowledgements

I would like to express my deepest gratitude to several individuals whose support was invaluable not only during the writing of my master's thesis but also in shaping who I am today.

First and foremost, I am deeply grateful to my girlfriend, Giorgia. Her unwavering support, patience, and encouragement have been the bedrock of my life during the development of this thesis. Her understanding and love, particularly during the most challenging times, have been instrumental in my success. I am truly blessed to have her by my side.

I am profoundly grateful to my family for their endless support and belief in my abilities, which have been a cornerstone of my academic journey. To my mother, thank you for instilling important moral values in me and showing me the greatest example of happiness; these principles have guided me every step of the way. My father deserves special thanks for his constant support and sage advice, which have been crucial in my decisions and progress. To my sister, thank you for setting an exemplary path to follow and for your invaluable advice. To my brother, thank you for the inspiration and the lively discussions that have motivated me to strive for excellence. To my 'Nonna,' thank you for all your stories and the values you shared; they have been a source of wisdom and guidance. My extended family's encouragement and confidence in me have also been a source of strength and motivation.

My friends have provided a network of advice, support, and relief from the daily grind. Their companionship has been a sanctuary, and I am eternally grateful for that. Special thanks to Andrea, who has always been there for me and is available for a call anytime. Also, to Anna, who has been a constant presence since middle school and whose advice has been pivotal in shaping who I am today. I am also deeply thankful to Alessandro, Vincenzo, and Rino, who have been great supporters in tougher times and can always make me smile. Special thanks to Tancredi, the first person I met in high school, who has been a source of advice and a friend with whom to share lifelong memories through our travels.

I would also like to acknowledge Comala, the study room that has not only been my refuge but has also provided me with a productive environment and the

opportunity to forge new connections. The conducive atmosphere and the people it allowed me to meet have been instrumental in my academic pursuits and personal development, providing a space for focused work and fruitful interactions.

Special thanks are due to my thesis advisors, Natasha, Daniela, Bisma and Giorgio, whose guidance and expertise have been instrumental in shaping the direction and execution of this research. Their invaluable input and direction have significantly contributed to the quality and depth of this thesis. I am also deeply grateful to Jenna, who made this double degree program possible and helped me find a way to move in with my girlfriend here in Chicago—something I would have never expected and for which I am incredibly thankful.

This thesis stands as a milestone in my academic career, and these individuals have played a substantial part in helping me reach this stage. I am immensely thankful to everyone who supported me along the way.

*Simone*

# Table of Contents

List of Tables	VII
List of Figures	VIII
Acronyms	X
<b>1 Introduction</b>	<b>1</b>
1.1 Notation Convention . . . . .	1
1.2 Concepts and Background . . . . .	2
1.2.1 Bayesian Cramér-Rao Bound . . . . .	2
1.2.2 Communication Rate and Mutual Information . . . . .	3
1.2.3 Von Mises Distribution . . . . .	3
1.2.4 Steering Vectors and MIMO Antennas . . . . .	3
1.3 Goals of Dissertation . . . . .	4
<b>2 Previous Work</b>	<b>5</b>
<b>3 System Model</b>	<b>8</b>
3.1 Channel Model . . . . .	9
3.2 Sensing Task . . . . .	10
3.3 Communication Task . . . . .	10
3.4 ISAC Region . . . . .	10
<b>4 Fundamental Quantities for the Characterization of ISAC Scheme</b>	<b>12</b>
4.1 Bayesian Cramér-Rao Bound for Two Targets . . . . .	12
4.2 Optimal Communication and Sensing Points . . . . .	16
4.2.1 Optimal Sensing Point . . . . .	16
4.2.2 Optimal Communication Point . . . . .	16
4.3 Ways to Characterize the ISAC Region . . . . .	17

<b>5</b>	<b>Achievable Transmission Strategies for Characterization of ISAC Tradeoff</b>	<b>19</b>
5.1	General Communicating Strategy to the UE . . . . .	19
5.1.1	Communication Rate for Given Strategy . . . . .	20
5.1.2	BCRB for Given Strategy . . . . .	20
5.2	Strategy 1: One Information Carrying Beam . . . . .	20
5.2.1	Choice 1: Spanning among the two main eigenvectors of $\overline{\mathbf{M}}_1$ , and the two main eigenvectors of $\overline{\mathbf{M}}_2$ . . . . .	21
5.2.2	Choice 2: Spanning among the Directions of the Optimal Sensing and the Direction of Optimal Communication . . . . .	21
5.3	Strategy 2: One Information-less Beam . . . . .	21
5.3.1	Choice 1: Spanning among the two main eigenvectors of $\overline{\mathbf{M}}_1$ , and the two main eigenvectors of $\overline{\mathbf{M}}_2$ . . . . .	22
5.3.2	Choice 2: Spanning among the main eigenvector of $\overline{\mathbf{M}}_1$ , the main eigenvector of $\overline{\mathbf{M}}_2$ and the Directions of Optimal Sensing . . . . .	22
5.4	Strategy 3: Both One Information Carrying Beam and One Information- less Beam . . . . .	22
5.4.1	Choice 1: Spanning among the main eigenvector of $\overline{\mathbf{M}}_1$ , the main eigenvector of $\overline{\mathbf{M}}_2$ and the Direction of Optimal Communication . . . . .	23
5.4.2	Choice 2: Spanning among the Directions of the Optimal Sensing and the Direction of Optimal Communication . . . . .	23
5.4.3	Choice 3: Spanning among the main eigenvector of $\overline{\mathbf{M}}_1$ , the main eigenvector of $\overline{\mathbf{M}}_2$ , the Directions of the Optimal Sensing, and the Direction of Optimal Communication . . . . .	24
<b>6</b>	<b>Simulation Results</b>	<b>25</b>
6.1	Strategy 1: One Information Carrying Beam . . . . .	26
6.1.1	Choice 1: Spanning among the two main eigenvectors of $\overline{\mathbf{M}}_1$ , and the two main eigenvectors of $\overline{\mathbf{M}}_2$ . . . . .	26
6.1.2	Choice 2: Spanning among the Directions of the Optimal Sensing and the Direction of Optimal Communication . . . . .	29
6.2	Strategy 2: One Information-less Beam . . . . .	29
6.2.1	Choice 1: Spanning among the two main eigenvectors of $\overline{\mathbf{M}}_1$ , and the two main eigenvectors of $\overline{\mathbf{M}}_2$ . . . . .	29
6.2.2	Choice 2: Spanning among the main eigenvector of $\overline{\mathbf{M}}_1$ , the main eigenvector of $\overline{\mathbf{M}}_2$ and the Directions of Optimal Sensing . . . . .	33
6.3	Strategy 3: Both One Information Carrying Beam and One Information- less Beam . . . . .	33

6.3.1	Choice 1: Spanning among the main eigenvector of $\overline{\mathbf{M}}_1$ , the main eigenvector of $\overline{\mathbf{M}}_2$ and the Direction of Optimal Communication . . . . .	35
6.3.2	Choice 2: Spanning among the Directions of the Optimal Sensing and the Direction of Optimal Communication . . . .	35
6.3.3	Choice 3: Spanning among the main eigenvector of $\overline{\mathbf{M}}_1$ , the main eigenvector of $\overline{\mathbf{M}}_2$ , the Directions of the Optimal Sensing, and the Direction of Optimal Communication . . .	39
<b>7</b>	<b>Conclusion</b>	<b>42</b>
<b>A</b>	<b>Matlab Code</b>	<b>44</b>
	<b>Bibliography</b>	<b>56</b>

# List of Tables

6.1 Parameters Used to Compare Different Strategies . . . . .	25
---	----



# List of Figures

3.1	Representation of setting considered in this dissertation, with one communication target (end-user) and one sensing target. . . . .	8
6.1	First Strategy, First Direction Choice, BCRB-Rate Simulated Points.	26
6.2	First Strategy, First Direction Choice, BCRB-Rate Theoretical Points.	27
6.3	First Strategy, First Direction Choice, Total BCRB-Rate Simulated Points. . . . .	27
6.4	First Strategy, First Direction Choice, Total BCRB-Rate Theoretical Points. . . . .	28
6.5	First Strategy, First Direction Choice, Total BCRB-Rate Outer Bound.	28
6.6	First Strategy, Second Direction Choice, BCRB-Rate Simulated Points.	29
6.7	First Strategy, Second Direction Choice, BCRB-Rate Theoretical Points. . . . .	30
6.8	First Strategy, Second Direction Choice, Total BCRB-Rate Simulated Points. . . . .	30
6.9	First Strategy, Second Direction Choice, Total BCRB-Rate Theoretical Points. . . . .	31
6.10	First Strategy, Second Direction Choice, Total BCRB-Rate Outer Bound. . . . .	31
6.11	First Strategy, Comparison of Direction Choice, Total BCRB-Rate Outer Bound. . . . .	32
6.12	Second Strategy, First Direction Choice, BCRB-Rate Simulated Points.	33
6.13	Second Strategy, Second Direction Choice, BCRB-Rate Simulated Points. . . . .	34
6.14	Third Strategy, First Direction Choice, BCRB-Rate Simulated Points.	35
6.15	Third Strategy, First Direction Choice, Total BCRB-Rate Simulated Points. . . . .	36
6.16	Third Strategy, First Direction Choice, Total BCRB-Rate Outer Bound. . . . .	36
6.17	Third Strategy, Second Direction Choice, BCRB-Rate Simulated Points. . . . .	37

6.18	Third Strategy, Second Direction Choice, Total BCRB-Rate Simulated Points. . . . .	37
6.19	Third Strategy, Second Direction Choice, Total BCRB-Rate Outer Bound. . . . .	38
6.20	Third Strategy, Third Direction Choice, BCRB-Rate Simulated Points. . . . .	39
6.21	Third Strategy, Third Direction Choice, Total BCRB-Rate Simulated Points. . . . .	40
6.22	Third Strategy, Third Direction Choice, Total BCRB-Rate Outer Bound. . . . .	40
6.23	Third Strategy, Comparison of Direction Choice, Total BCRB-Rate Outer Bound. . . . .	41
6.24	First and Third Strategy, Comparison of Direction Choice, Total BCRB-Rate Outer Bound. . . . .	41

# Acronyms

**ISAC**

Integrated Sensing And Communication

**MIMO**

Multiple Input Multiple Output

**CRB**

Cramér-Rao Bound

**BCRB**

Bayesian Cramér-Rao Bound

**bpcu**

Bits per Channel Use

**pdf**

Probability Density Function

**LoS**

Line of Sight

**MI**

Mutual Information

**BS**

Base Station

**EU**

End User

**UE**

User Equipment

**ULA**

Uniform Linear Antenna

**i.i.d.**

Independent and Identically Distributed

**BFIM**

Bayesian Fisher Information Matrix

# Chapter 1

## Introduction

Integrated Sensing and Communication (ISAC) is emerging as a critical technology for future wireless networks, blending sensing and communication to efficiently utilize spectrum and hardware resources. This convergence is driven by the demands of applications such as autonomous vehicles and immersive technologies, alongside advancements in millimeter wave and massive MIMO technologies. ISAC promises to mitigate spectrum congestion and enhance spectral, energy, and economic efficiencies. While initial research has focused on practical ISAC system designs, understanding the theoretical limits of ISAC is crucial for bridging the gap between current capabilities and potential performance peaks. This involves exploring the trade-offs between sensing and communication functions to guide the development of more effective ISAC solutions. As a cornerstone of next-generation networks, ISAC represents a synergistic approach that significantly boosts both sensing and communication capabilities, ensuring the adaptability and efficiency of future wireless systems.

Extensive research has been done on the fundamental tradeoff of ISAC [1] under the assumption of known state information from a communication point of view. This is, however, non-realistic as channels often change and need to be continuously estimated.

We start by reviewing the literature on ISAC and related topics used in this dissertation. The model on which we focus is then shown and presented. We proceed with a detailed explanation of what has been done to achieve the results, which are commented on in the end.

### 1.1 Notation Convention

We denote with  $a$ ,  $\mathbf{a}$ , and  $\mathbf{A}$  scalar random variables, random vectors, and random matrices, respectively. With  $A$ , we denote known quantities, e.g.,  $P$  is the power.

With  $\mathbb{E}_{\mathbf{x}}\{\cdot\}$ , we denote the expected value of the argument with respect to  $\mathbf{x}$ . With  $\text{tr}\{\cdot\}$ , we denote the trace of a (square) matrix. We use  $|\cdot|$  for the absolute value of a scalar and  $\|\cdot\|_p$  for the  $l_p$  norm of a vector which is the Euclidean norm when the subscript is omitted. With  $\text{diag}(\mathbf{b})$ , we denote a diagonal matrix with  $\mathbf{b}$  being its diagonal. The notations  $[\cdot]^*$  and  $[\cdot]^H$  are used to indicate the complex conjugate and the Hermitian transpose of the argument, respectively. We denote with  $\Re\{\cdot\}$  and  $\Im\{\cdot\}$  the operators returning their argument's real and imaginary parts, respectively. The notation  $\mathbb{C}^{M \times N}$  denotes the set of complex-valued matrices with  $M$  rows and  $N$  columns. The notation  $\hat{\mathbf{a}}$ , denotes the unit norm vector obtained by dividing the vector  $\mathbf{a}$  by its norm.

## 1.2 Concepts and Background

This section will present the main concepts needed to understand this dissertation, with a short theoretical explanation.

### 1.2.1 Bayesian Cramér-Rao Bound

The Cramér-Rao Bound (CRB) is a lower bound on the variance ( $\text{Var}\{\cdot\}$ ) of any unbiased parameter estimator [2]. In simpler terms, it tells us the best accuracy we can achieve when estimating a parameter from noisy observations. Mathematically, for an unbiased estimator  $\hat{\theta}$  of a parameter  $\theta$ , the CRB states that:

$$\text{Var}(\hat{\theta}) \geq \frac{1}{I(\theta)}, \quad (1.1)$$

where  $I(\theta)$  is the Fisher Information and can be computed as:

$$\mathcal{I}(\theta) = -\mathbb{E} \left[ \frac{\partial^2 \log L(\theta)}{\partial \theta^2} \right], \quad (1.2)$$

where  $L(\theta)$  is likelihood function.

The Bayesian Cramér-Rao Bound (BCRB) [3] can be used when prior information about the parameter is available. This bound incorporates both the prior distribution of the parameter and the likelihood of the observations, giving a more general lower bound on the estimator's variance. It integrates over all possible values of the parameter:

$$\mathbb{E}[(\hat{\theta} - \theta)^2] \geq \left( \mathbb{E} \left[ \frac{\partial^2}{\partial \theta^2} \ln p(y|\theta) \right] + \mathbb{E} \left[ \frac{\partial^2}{\partial \theta^2} \ln p(\theta) \right] \right)^{-1}, \quad (1.3)$$

where  $p(y|\theta)$  is the likelihood function and  $p(\theta)$  is the prior distribution.

## 1.2.2 Communication Rate and Mutual Information

The communication rate is the rate at which information can be transmitted over a communication channel, usually measured in bits per channel use (bpcu). It is constrained by the channel capacity, which can be found by maximizing the mutual information between the transmitted and received signal.

Mutual information measures the amount of information one random variable contains about another [4]. In the context of communication, it quantifies the amount of information transmitted from the sender to the receiver. For a channel with input  $X$  and output  $Y$ , the mutual information  $I(X; Y)$  is given by:

$$I(X; Y) = h(X) - h(X|Y) \quad (1.4)$$

where  $h(X)$  is the differential entropy of  $X$  and  $h(X|Y)$  is the conditional differential entropy of  $X$  given  $Y$ . The differential entropy can be defined as:

$$h(X) = - \int_{-\infty}^{\infty} f_X(x) \log f_X(x) dx, \quad (1.5)$$

where  $f_X(x)$  is the pdf of  $X$ .

## 1.2.3 Von Mises Distribution

The Von Mises Distribution [5] is a probability distribution for circular data analogous to the normal distribution for linear data. It is used when dealing with angles or periodic phenomena. The probability density function (pdf) of the Von Mises distribution is:

$$f(\theta; \mu, \kappa) = \frac{e^{\kappa \cos(\theta - \mu)}}{2\pi I_0(\kappa)}, \quad (1.6)$$

where  $\mu$  is the mean direction,  $\kappa$  is the concentration parameter (analogous to the inverse of the variance), and  $I_0(\kappa)$  is the modified Bessel function of the first kind. The support of the pdf is an interval of length  $2\pi$  centered at  $\mu$ . Note that  $1/\kappa$  plays a role similar to  $\sigma^2$  (the variance) in the Gaussian distribution.

The von Mises distribution is particularly useful for modeling data that are directional or cyclical, such as phases, angles, or the time of day.

## 1.2.4 Steering Vectors and MIMO Antennas

Steering Vectors are used in array signal processing to describe the phase shifts required to steer the beam of an antenna array toward a specific direction. In a far-field Line-of-Sight (LoS) MIMO model [6], the steering vector  $\mathbf{a}(\theta)$  for a direction  $\theta$  is usually defined by:

$$\mathbf{a}(\theta) = \frac{1}{\sqrt{M}} \left[ 1, e^{jkd \cos(\theta)}, e^{j2kd \cos(\theta)}, \dots, e^{j(M-1)kd \cos(\theta)} \right]^T, \quad (1.7)$$

where  $k$  is the wavenumber,  $d$  is the distance between antennas, and  $M$  is the number of antennas. This normalization by  $\sqrt{M}^{-1}$  ensures that the steering vector has unit length.

Note that the steering vectors of an antenna with  $M$  elements, where  $M = 2\tilde{M} + 1$ , can be written with indexes  $n \in \{-\tilde{M}, -\tilde{M} + 1, \dots, \tilde{M} - 1, \tilde{M}\}$ . Namely:

$$\mathbf{a}(\theta) = \frac{1}{\sqrt{M}} \left[ e^{j(-\tilde{M})kd \cos(\theta)}, e^{j(-\tilde{M}+1)kd \cos(\theta)}, \dots, 1, \dots, e^{j(\tilde{M})kd \cos(\theta)} \right]^T. \quad (1.8)$$

This formulation above ensures the orthogonality between the steering vector and its derivative,  $\dot{\mathbf{a}}^H(\theta)\mathbf{a}(\theta) = 0$ .

Multiple-input multiple-output (MIMO) systems use multiple antennas at both the transmitter and receiver to improve communication performance. MIMO technology exploits spatial diversity and spatial multiplexing to increase data rates and reliability.

### 1.3 Goals of Dissertation

This dissertation aims to study the fundamental limits of ISAC systems under a specific set of assumptions. In particular, we focus on deriving the BCRB for the joint estimation of two targets. We then proceed with the study of the optimal sensing and communication points. Finally, we study various transmission strategies to achieve an inner bound for the BCRB-Rate region and identify the ISAC tradeoff in our scenario.

We attempt to obtain similar results as in [1] in a more realistic scenario. Hence, we communicate with targets that must be sensed and assume only partially known channel state information at the receiver. A Base Station (BS) estimates the angle of arrivals of targets in the vicinity. Already acquired targets are communication receivers, while other targets may appear on the scene and thus must be estimated and characterized by different prior distributions. Our goal is to derive the fundamental Rate-BCRB tradeoff region.

Under these different assumptions, we study the new tradeoffs in the system, proposing a simple outer bound and several communication strategies to achieve some inner bounds.



## Chapter 2

# Previous Work

The state-of-the-art ISAC reflects a variety of approaches, ranging from theoretical foundations to practical implementations and standards. The conceptualization of ISAC can be traced back to the necessity for coexistence and coordination between radar and communication systems within the same spectral resources. Early works focused on understanding and defining the potential synergies between these functionalities. Paper [7] provides an extensive review of the fundamental limits of ISAC, exploring how traditional radio sensing and emerging ISAC approaches can be unified under a comprehensive framework. Similarly, the work in [8] delineates a novel relationship between mutual information and the minimum mean-square error in Gaussian channels. This fundamental concept underpins the theoretical limits of ISAC performance.

As we transition from 5G to 6G, ISAC is identified as a key technology that exploits dense cellular infrastructures to create highly perceptive networks. Paper [9] highlights how ISAC could integrate within 6G networks, enhancing both the performance and functionality of RANs by incorporating sensing capabilities. This vision aligns with the trends in IoT, where ISAC could redefine the architectural layers. Paper [10] discusses the transition towards a unified signaling layer in IoT, driven by ISAC technologies, indicating a shift towards more integrated and efficient network frameworks. Practical implementations of ISAC have been explored in various domains, including vehicular networks and cooperative systems. Paper [11] introduces a predictive beamforming approach in vehicular networks, showcasing how ISAC can effectively reduce overhead while improving the accuracy of vehicle localization and communication. This application demonstrates the practical benefits and efficiency gains from deploying ISAC in dynamic environments.

ISAC can be broadly classified into two categories: device-free ISAC and device-based ISAC [7]. In device-free ISAC, the sensing targets cannot transmit or receive signals, or the sensing procedure does not rely on the target's transmit/receive capabilities. A typical example is radar sensing, where a radar transmits a probing

signal, and the echo reflected from the target is used for sensing. In device-based ISAC, the sensing functionality is achieved by device-based sensing, where the sensing targets can transmit and receive signals. A common example is localization and communication in cellular networks.

Despite the promising advances, ISAC still faces significant challenges, particularly in balancing the dual-functional performance and optimizing resource allocation. The research highlighted in [10] and [7] identifies these challenges and proposes future research directions, including the development of more sophisticated integration techniques and the exploration of optimal trade-offs between sensing and communication capabilities. We focus on the latter problem studied in [1] under the model of having some targets to sense and others to communicate with under known state information at both the transmitter and receiver. The theoretical studies allow us to understand the limits one can try to achieve in practical scenarios. For this reason, we try to fill the gap in the literature caused by the lack of more realistic settings.

The work in [1], which we will reference the most, stands as one of the first to address the fundamental trade-off in ISAC from both information-theoretic and estimation-theoretic perspectives. It demonstrates that the optimal sensing performance is achieved when the sample covariance matrix  $\mathbf{R}_{\mathbf{X}} = \frac{1}{T}\mathbf{X}\mathbf{X}^H$  has a deterministic trace, and the distribution  $p(\mathbf{R}_{\mathbf{X}})$  (and hence  $p(\mathbf{X})$ ) is restricted to the optimal solution set of a deterministic CRB minimization problem. If the solution is unique, the sensing-optimal sample covariance matrix  $\mathbf{R}_{\mathbf{X}}$  itself should be deterministic. The authors define the CRB-rate region as the set of all achievable communication rate and sensing CRB pairs. They propose a pentagon inner bound of the CRB-rate region that can be achieved through a simple time-sharing strategy. Within this framework, they study ISAC performance at the two corner points of the CRB-rate region:  $P_{CS}$  (minimum achievable CRB constrained by maximum communication rate) and  $P_{SC}$  (maximum achievable communication rate constrained by minimum CRB). The paper derives the high-SNR communication capacity for the sensing-optimal point  $P_{SC}$ . It proves that it can be asymptotically achieved by a strategy based on uniform sampling over the set of semi-unitary matrices (the Stiefel manifold). Additionally, they provide lower and upper bounds for the sensing CRB at the communication-optimal point  $P_{CS}$ . The paper reveals a two-fold trade-off in ISAC systems:

- Subspace Trade-Off (ST): Balances resource allocation between the subspaces spanned by sensing and communication channels.
- Deterministic-Random Trade-Off (DRT): Depicts the exploitable degrees of freedom (DoFs) in ISAC signals.

The authors propose an outer bound and various inner bounds for the CRB-rate region based on these trade-offs. We will expand upon their work by changing

the assumptions made on the model, considering an incomplete knowledge of the channel state information. We also consider a case with two targets to be jointly sensed, where one of the two is also a communication target. By studying this new setting, we provide a step forward to completely understanding ISAC tradeoff and its limits in real-life scenarios.

# Chapter 3

## System Model

For the sake of simplicity, we consider a two-dimensional (i.e., no  $z$ -coordinate) scenario with one communication target and one additional separate sensing target, as illustrated in Fig. 3.1.

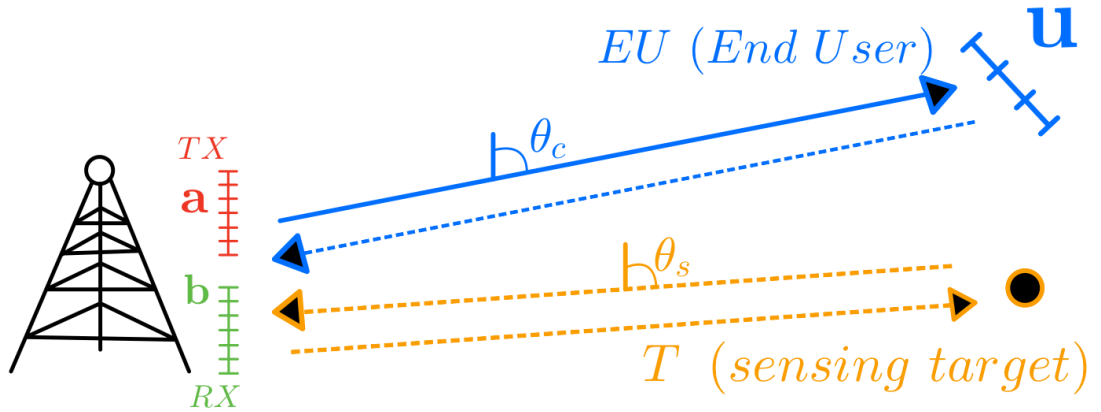


**Figure 3.1:** Representation of setting considered in this dissertation, with one communication target (end-user) and one sensing target.

The Base Station (BS) is simultaneously a transmitter for the communication receivers and a mono-static radar for the sensing targets. The BS comprises a transmitting uniform linear antenna array (ULA) with  $M_{\text{TX}}$  elements, characterized by the steering vector  $\mathbf{a} \in \mathbb{C}^{M_{\text{TX}} \times 1}$ , and a receiving ULA with  $M_{\text{RX}}$  elements, characterized by the steering vector  $\mathbf{b} \in \mathbb{C}^{M_{\text{RX}} \times 1}$ . The BS operates in full-duplex mode. We make the idealized assumption that there is no self-interference on the TX side from the RX side. Future work will investigate even more realistic scenarios.

The communication receiver, or UE for ‘user equipment,’ has a ULA with  $M_{\text{UE}}$  elements, characterized by the steering vector  $\mathbf{u} \in \mathbb{C}^{M_{\text{UE}} \times 1}$ . The UE reflects the BS-transmit signal back to the BS-receiver, which enables it to estimate their angle of arrival.

### 3.1 Channel Model

The BS transmits signal is denoted by  $\mathbf{X} \in \mathbb{C}^{M_{\text{TX}} \times T}$ , where  $T$  is the channel coherence time. We assume the sensing parameters vary synchronously with the communication channel parameters every  $T$  channel uses. At the same time, the BS receives the signal  $\mathbf{Y}_s \in \mathbb{C}^{M_{\text{RX}} \times T}$  from the reflections of targets and objects present in the surroundings. The UE receives the signal  $\mathbf{Y}_c \in \mathbb{C}^{M_{\text{UE}} \times T}$ . We write the received signals as

$$\mathbf{Y}_c = \mathbf{H}_c \mathbf{X} + \mathbf{Z}_c, \quad \mathbf{H}_c = \alpha \mathbf{u}(\theta_1) \mathbf{a}^H(\theta_1), \quad (3.1)$$

$$\mathbf{Y}_s = \mathbf{H}_s \mathbf{X} + \mathbf{Z}_s, \quad \mathbf{H}_s = \sum_{\ell=1}^{N_s} \beta_\ell \mathbf{b}(\theta_\ell) \mathbf{a}^H(\theta_\ell), \quad (3.2)$$

where:

- $\mathbf{X} \in \mathbb{C}^{M_{\text{TX}} \times T}$  is the transmit signal subject to

$$\mathbb{E} \{ \text{tr} \{ \mathbf{R}_\mathbf{X} \} \} \leq P_{\text{TX}} M_{\text{TX}}, \quad (3.3)$$

where  $\mathbf{R}_\mathbf{X} := T^{-1} \mathbf{X} \mathbf{X}^H$  is the ‘sample covariance matrix.’ Note that  $P_{\text{TX}}$  has the meaning of average power constraint per transmit antenna.

- $\mathbf{Z}_c$  has entries assumed i.i.d., circularly symmetric, complex Gaussian, with zero mean and variance  $\sigma_c^2$ .
- $\mathbf{Z}_s$  has entries assumed i.i.d., circularly symmetric, complex Gaussian, with zero mean and variance  $\sigma_s^2$ .
- $\mathbf{H}_c \in \mathbb{C}^{M_{\text{UE}} \times M_{\text{TX}}}$  is the down-link communication channel matrix.  $\theta_1 \in [0, 2\pi]$  denotes the angle of arrival of the transmit signal, and  $\alpha \in \mathbb{C}$  is the channel attenuation, both assumed perfectly known at the UE.
- $\mathbf{H}_s \in \mathbb{C}^{M_{\text{RX}} \times M_{\text{TX}}}$  is the sensing channel matrix, where  $N_s$  is the number of sensing targets, assumed known at the BS. The angles of arrival  $(\theta_1, \theta_2, \dots, \theta_{N_s}) \in [0, 2\pi]^{N_s}$  must be estimated.  $(\beta_1, \beta_2, \dots, \beta_{N_s}) \in \mathbb{C}^{N_s}$  is the vector of channel gains from the targets to the BS. We assume that the prior distribution on the target parameters factorizes as

$$P_{\theta_1, \theta_2, \dots, \theta_{N_s}, \beta_1, \beta_2, \dots, \beta_{N_s}} = \prod_{\ell=1}^{N_s} P_{\theta_\ell} P_{\Re\{\beta_\ell\}} P_{\Im\{\beta_\ell\}}. \quad (3.4)$$

## 3.2 Sensing Task

The sensing task consists in estimating the angle of arrivals in  $\mathbf{H}_s$  in (3.2). As a metric for this sensing task, we use the BCRB [1], a lower bound for the Mean Squared Error (MSE) of weakly unbiased estimators. The BCRB is defined as

$$\epsilon := \mathbb{E}_{\mathbf{X}} \left\{ \text{tr} \left\{ \mathbf{J}_{\boldsymbol{\theta}|\mathbf{X}}^{-1} \right\} \right\}, \quad (3.5)$$

where  $\mathbf{J}_{\boldsymbol{\theta}|\mathbf{X}}$  is the Bayesian Fisher Information Matrix (BFIM) of the parameters we wish to estimate. The BFIM of the parameters  $\boldsymbol{\theta}$ , is given by [12]:

$$\begin{aligned} \mathbf{J}_{\boldsymbol{\theta}|\mathbf{X}} := & \mathbb{E} \left\{ \frac{\partial \ln p_{\mathbf{Y}_s|\mathbf{X},\boldsymbol{\theta}}(\mathbf{Y}_s | \mathbf{X}, \boldsymbol{\theta})}{\partial \boldsymbol{\theta}} \frac{\partial \ln p_{\mathbf{Y}_s|\mathbf{X},\boldsymbol{\theta}}(\mathbf{Y}_s | \mathbf{X}, \boldsymbol{\theta})}{\partial \boldsymbol{\theta}^T} \middle| \mathbf{X} \right\} \\ & + \mathbb{E} \left\{ \frac{\partial \ln p_{\boldsymbol{\theta}}(\boldsymbol{\theta})}{\partial \boldsymbol{\theta}} \frac{\partial \ln p_{\boldsymbol{\theta}}(\boldsymbol{\theta})}{\partial \boldsymbol{\theta}^T} \right\}. \end{aligned} \quad (3.6)$$

## 3.3 Communication Task

The communication task consists of reliably transmitting information to the UE with received signal  $\mathbf{Y}_c$  in (3.1). As a metric for this communication task, we use the ergodic achievable rate: [1]

$$R := \frac{1}{T} I(\mathbf{X}; \mathbf{Y}_c | \mathbf{H}_c), \text{ s.t. } \mathbb{E} \{ \text{tr} \{ \mathbf{R}_{\mathbf{X}} \} \} \leq P_{\text{TX}} M_{\text{TX}}. \quad (3.7)$$

Note that the channel  $\mathbf{H}_c$  is a random variable with known prior distribution; hence the expected value implied by the definition of mutual information is to be considered with respect to the prior probability density function of  $\mathbf{H}_c$ .

## 3.4 ISAC Region

Overall, we are interested in obtaining the lowest possible estimation error and the highest possible rate. The minimum sensing error is obtained by minimizing (3.5) with respect to the pdf of the transmit signal  $\mathbf{X}$ . On the other hand, the maximum achievable rate is obtained by maximizing (3.7) with respect to the pdf of the transmit signal  $\mathbf{X}$ . These two tasks are conflicting, so we define the ISAC region where the power constraint on  $\mathbf{X}$  is introduced.

The ISAC region is defined as the set of achievable pairs  $(\epsilon, R)$ , where  $\epsilon$  is the BCRB for the joint estimation of all the angles we need to estimate, and  $R$  is the

ergodic communication rate. This region can be mathematically expressed as:

$$\mathcal{R}_{\text{ISAC}} = \bigcup_{p_{\mathbf{X}}(\mathbf{X}) \in \mathcal{X}(P_{\text{TX}}M_{\text{TX}})} \left\{ (\epsilon, R) \mid \epsilon = \mathbb{E}_{\mathbf{X}} \left\{ \text{tr} \left\{ \mathbf{J}_{\theta|\mathbf{X}}^{-1} \right\} \right\}, R = \frac{1}{T} I(\mathbf{X}; \mathbf{Y}_c | \mathbf{H}_c) \right\} \quad (3.8)$$

where  $\mathcal{X}(P_{\text{TX}}M_{\text{TX}})$  is the set of all possible distributions for the input signal that meet the average power constraint  $P_{\text{TX}}M_{\text{TX}}$ , i.e.,  $\mathbb{E} \{ \text{tr} \{ \mathbf{R}_{\mathbf{X}} \} \} \leq P_{\text{TX}}M_{\text{TX}}$ .

## Chapter 4

# Fundamental Quantities for the Characterization of ISAC Scheme

In this chapter, we dive deeper into the definition of the errors for the joint estimation of two targets and the general formulation of the communication rate. A general form was derived in [13]; here, we apply the general results to obtain the case of interest of two targets.

### 4.1 Bayesian Cramér-Rao Bound for Two Targets

It is key for our study to evaluate the BCRB for the joint estimation of the unknowns in the sensing channel matrix: the angles and the complex amplitudes. We start by defining the following quantities based on the parameters in (3.2):

$$\mathbf{B} = [\mathbf{b}(\theta_1) \quad \mathbf{b}(\theta_2)], \quad \mathbf{A} = [\mathbf{a}(\theta_1) \quad \mathbf{a}(\theta_2)], \quad (4.1)$$

$$\boldsymbol{\theta} = [\theta_1 \quad \theta_2]^\top, \quad \boldsymbol{\beta} = [\beta_1 \quad \beta_2]^\top, \quad \boldsymbol{\mathcal{B}} = \text{diag}(\boldsymbol{\beta}). \quad (4.2)$$

We also define

$$\dot{\mathbf{B}} = \left[ \frac{\partial \mathbf{b}(\theta_1)}{\partial \theta_1} \quad \frac{\partial \mathbf{b}(\theta_2)}{\partial \theta_2} \right], \quad \dot{\mathbf{A}} = \left[ \frac{\partial \mathbf{a}(\theta_1)}{\partial \theta_1} \quad \frac{\partial \mathbf{a}(\theta_2)}{\partial \theta_2} \right]. \quad (4.3)$$

According to [13], we can write the Fisher Information matrix as

$$\mathbf{F} = 2 \begin{bmatrix} \Re(\mathbf{F}_{11}) & \Re(\mathbf{F}_{12}) & -\Im(\mathbf{F}_{12}) \\ \Re^\top(\mathbf{F}_{12}) & \Re(\mathbf{F}_{22}) & -\Im(\mathbf{F}_{22}) \\ -\Im^\top(\mathbf{F}_{12}) & -\Im^\top(\mathbf{F}_{22}) & \Re(\mathbf{F}_{22}) \end{bmatrix}, \quad (4.4)$$



where

$$\begin{aligned} \mathbf{F}_{11} = & \frac{T}{\sigma^2} (\dot{\mathbf{B}}^H \dot{\mathbf{B}}) \odot (\mathcal{B}^* \mathbf{A}^H \mathbf{R}_X^* \mathbf{A} \mathcal{B}) + \frac{T}{\sigma^2} (\dot{\mathbf{B}}^H \mathbf{B}) \odot (\mathcal{B}^* \mathbf{A}^H \mathbf{R}_X^* \dot{\mathbf{A}} \mathcal{B}) \\ & + \frac{T}{\sigma^2} (\mathbf{B}^H \dot{\mathbf{B}}) \odot (\mathcal{B}^* \dot{\mathbf{A}}^H \mathbf{R}_X^* \mathbf{A} \mathcal{B}) + \frac{T}{\sigma^2} (\mathbf{B}^H \mathbf{B}) \odot (\mathcal{B}^* \dot{\mathbf{A}}^H \mathbf{R}_X^* \dot{\mathbf{A}} \mathcal{B}), \end{aligned} \quad (4.5)$$

$$\mathbf{F}_{12} = \frac{T}{\sigma^2} (\dot{\mathbf{B}}^H \mathbf{B}) \odot (\mathcal{B}^* \mathbf{A}^H \mathbf{R}_X^* \mathbf{A}) + \frac{T}{\sigma^2} (\mathbf{B}^H \dot{\mathbf{B}}) \odot (\mathcal{B}^* \dot{\mathbf{A}}^H \mathbf{R}_X^* \mathbf{A}), \quad (4.6)$$

$$\mathbf{F}_{22} = \frac{T}{\sigma^2} (\mathbf{B}^H \mathbf{B}) \odot (\mathbf{A}^H \mathbf{R}_X^* \mathbf{A}). \quad (4.7)$$

For clarity, we simplify the notation during the derivation by using  $\mathbf{b}_1 = \mathbf{b}(\theta_1)$ ,  $\mathbf{b}_2 = \mathbf{b}(\theta_2)$ ,  $\mathbf{a}_1 = \mathbf{a}(\theta_1)$  and  $\mathbf{a}_2 = \mathbf{a}(\theta_2)$ . We can thus write:

$$\begin{aligned} \mathbf{F}_{11} = & \frac{T}{\sigma^2} \begin{bmatrix} \|\beta_1\|^2 & \beta_1^* \beta_2 \\ \beta_2^* \beta_1 & \|\beta_2\|^2 \end{bmatrix} \\ & \odot \left( \begin{bmatrix} \|\dot{\mathbf{b}}_1\|^2 & \dot{\mathbf{b}}_1^H \dot{\mathbf{b}}_2 \\ \dot{\mathbf{b}}_2^H \dot{\mathbf{b}}_1 & \|\dot{\mathbf{b}}_2\|^2 \end{bmatrix} \odot \begin{bmatrix} \mathbf{a}_1^H \mathbf{R}_X^* \mathbf{a}_1 & \mathbf{a}_1^H \mathbf{R}_X^* \mathbf{a}_2 \\ \mathbf{a}_2^H \mathbf{R}_X^* \mathbf{a}_1 & \mathbf{a}_2^H \mathbf{R}_X^* \mathbf{a}_2 \end{bmatrix} \right. \\ & + \begin{bmatrix} \dot{\mathbf{b}}_1^H \dot{\mathbf{b}}_1 & \dot{\mathbf{b}}_1^H \dot{\mathbf{b}}_2 \\ \dot{\mathbf{b}}_2^H \dot{\mathbf{b}}_1 & \dot{\mathbf{b}}_2^H \dot{\mathbf{b}}_2 \end{bmatrix} \odot \begin{bmatrix} \mathbf{a}_1^H \mathbf{R}_X^* \dot{\mathbf{a}}_1 & \mathbf{a}_1^H \mathbf{R}_X^* \dot{\mathbf{a}}_2 \\ \mathbf{a}_2^H \mathbf{R}_X^* \dot{\mathbf{a}}_1 & \mathbf{a}_2^H \mathbf{R}_X^* \dot{\mathbf{a}}_2 \end{bmatrix} \\ & + \begin{bmatrix} \mathbf{b}_1^H \dot{\mathbf{b}}_1 & \mathbf{b}_1^H \dot{\mathbf{b}}_2 \\ \mathbf{b}_2^H \dot{\mathbf{b}}_1 & \mathbf{b}_2^H \dot{\mathbf{b}}_2 \end{bmatrix} \odot \begin{bmatrix} \dot{\mathbf{a}}_1^H \mathbf{R}_X^* \mathbf{a}_1 & \dot{\mathbf{a}}_1^H \mathbf{R}_X^* \mathbf{a}_2 \\ \dot{\mathbf{a}}_2^H \mathbf{R}_X^* \mathbf{a}_1 & \dot{\mathbf{a}}_2^H \mathbf{R}_X^* \mathbf{a}_2 \end{bmatrix} \\ & \left. + \begin{bmatrix} \|\mathbf{b}_1\|^2 & \mathbf{b}_1^H \mathbf{b}_2 \\ \mathbf{b}_2^H \mathbf{b}_1 & \|\mathbf{b}_2\|^2 \end{bmatrix} \odot \begin{bmatrix} \dot{\mathbf{a}}_1^H \mathbf{R}_X^* \dot{\mathbf{a}}_1 & \dot{\mathbf{a}}_1^H \mathbf{R}_X^* \dot{\mathbf{a}}_2 \\ \dot{\mathbf{a}}_2^H \mathbf{R}_X^* \dot{\mathbf{a}}_1 & \dot{\mathbf{a}}_2^H \mathbf{R}_X^* \dot{\mathbf{a}}_2 \end{bmatrix} \right), \end{aligned} \quad (4.8)$$

$$\begin{aligned} \mathbf{F}_{12} = & \frac{T}{\sigma^2} \begin{bmatrix} \beta_1^* & 0 \\ 0 & \beta_2^* \end{bmatrix} \\ & \odot \left( \begin{bmatrix} \dot{\mathbf{b}}_1^H \mathbf{b}_1 & \dot{\mathbf{b}}_1^H \mathbf{b}_2 \\ \dot{\mathbf{b}}_2^H \mathbf{b}_1 & \dot{\mathbf{b}}_2^H \mathbf{b}_2 \end{bmatrix} \odot \begin{bmatrix} \mathbf{a}_1^H \mathbf{R}_X^* \mathbf{a}_1 & \mathbf{a}_1^H \mathbf{R}_X^* \mathbf{a}_2 \\ \mathbf{a}_2^H \mathbf{R}_X^* \mathbf{a}_1 & \mathbf{a}_2^H \mathbf{R}_X^* \mathbf{a}_2 \end{bmatrix} \right. \\ & \left. + \begin{bmatrix} \mathbf{b}_1^H \dot{\mathbf{b}}_1 & \mathbf{b}_1^H \dot{\mathbf{b}}_2 \\ \mathbf{b}_2^H \dot{\mathbf{b}}_1 & \mathbf{b}_2^H \dot{\mathbf{b}}_2 \end{bmatrix} \odot \begin{bmatrix} \dot{\mathbf{a}}_1^H \mathbf{R}_X^* \mathbf{a}_1 & \dot{\mathbf{a}}_1^H \mathbf{R}_X^* \mathbf{a}_2 \\ \dot{\mathbf{a}}_2^H \mathbf{R}_X^* \mathbf{a}_1 & \dot{\mathbf{a}}_2^H \mathbf{R}_X^* \mathbf{a}_2 \end{bmatrix} \right), \end{aligned} \quad (4.9)$$

$$\mathbf{F}_{22} = \frac{T}{\sigma^2} \begin{bmatrix} \mathbf{b}_1^H \mathbf{b}_1 & \mathbf{b}_1^H \mathbf{b}_2 \\ \mathbf{b}_2^H \mathbf{b}_1 & \mathbf{b}_2^H \mathbf{b}_2 \end{bmatrix} \odot \begin{bmatrix} \mathbf{a}_1^H \mathbf{R}_X^* \mathbf{a}_1 & \mathbf{a}_1^H \mathbf{R}_X^* \mathbf{a}_2 \\ \mathbf{a}_2^H \mathbf{R}_X^* \mathbf{a}_1 & \mathbf{a}_2^H \mathbf{R}_X^* \mathbf{a}_2 \end{bmatrix}. \quad (4.10)$$

We can further simplify the expressions using the Hermitian operation and

matrix properties. Then:

$$\begin{aligned}
 \mathbf{F}_{11} = & \frac{T}{\sigma^2} \begin{bmatrix} \|\beta_1\|^2 & \beta_1^* \beta_2 \\ \beta_2^* \beta_1 & \|\beta_2\|^2 \end{bmatrix} \\
 & \odot \left( \begin{bmatrix} \|\dot{\mathbf{b}}_1\|^2 & \dot{\mathbf{b}}_1^H \dot{\mathbf{b}}_2 \\ \dot{\mathbf{b}}_2^H \dot{\mathbf{b}}_1 & \|\dot{\mathbf{b}}_2\|^2 \end{bmatrix} \odot \begin{bmatrix} \mathbf{a}_1^H \mathbf{R}_X^* \mathbf{a}_1 & \mathbf{a}_1^H \mathbf{R}_X^* \mathbf{a}_2 \\ \mathbf{a}_2^H \mathbf{R}_X^* \mathbf{a}_1 & \mathbf{a}_2^H \mathbf{R}_X^* \mathbf{a}_2 \end{bmatrix} \right) \\
 & + \begin{bmatrix} 2\text{Re} \left\{ \dot{\mathbf{b}}_1^H \dot{\mathbf{b}}_1 \dot{\mathbf{a}}_1^H \mathbf{R}_X^* \mathbf{a}_1 \right\} & \dot{\mathbf{b}}_1^H \dot{\mathbf{b}}_2 \left( \dot{\mathbf{a}}_1^H \mathbf{R}_X^* \mathbf{a}_2 - \frac{\sin \theta_1}{\sin \theta_2} \mathbf{a}_1^H \mathbf{R}_X^* \dot{\mathbf{a}}_2 \right) \\ \dot{\mathbf{b}}_2^H \dot{\mathbf{b}}_1 \left( \dot{\mathbf{a}}_2^H \mathbf{R}_X^* \mathbf{a}_1 - \frac{\sin \theta_2}{\sin \theta_1} \mathbf{a}_2^H \mathbf{R}_X^* \dot{\mathbf{a}}_1 \right) & 2\text{Re} \left\{ \dot{\mathbf{b}}_2^H \dot{\mathbf{b}}_2 \dot{\mathbf{a}}_2^H \mathbf{R}_X^* \mathbf{a}_2 \right\} \end{bmatrix} \\
 & + \left( \begin{bmatrix} \|\mathbf{b}_1\|^2 & \mathbf{b}_1^H \mathbf{b}_2 \\ \mathbf{b}_2^H \mathbf{b}_1 & \|\mathbf{b}_2\|^2 \end{bmatrix} \odot \begin{bmatrix} \dot{\mathbf{a}}_1^H \mathbf{R}_X^* \dot{\mathbf{a}}_1 & \dot{\mathbf{a}}_1^H \mathbf{R}_X^* \dot{\mathbf{a}}_2 \\ \dot{\mathbf{a}}_2^H \mathbf{R}_X^* \dot{\mathbf{a}}_1 & \dot{\mathbf{a}}_2^H \mathbf{R}_X^* \dot{\mathbf{a}}_2 \end{bmatrix} \right), \tag{4.11}
 \end{aligned}$$

$$\mathbf{F}_{12} = \frac{T}{\sigma^2} \begin{bmatrix} \beta_1^* \left( \dot{\mathbf{b}}_1^H \mathbf{b}_1 \mathbf{a}_1^H \mathbf{R}_X^* \mathbf{a}_1 + \mathbf{b}_1^H \dot{\mathbf{b}}_1 \dot{\mathbf{a}}_1^H \mathbf{R}_X^* \mathbf{a}_1 \right) & 0 \\ 0 & \beta_2^* \left( \dot{\mathbf{b}}_2^H \mathbf{b}_2 \mathbf{a}_2^H \mathbf{R}_X^* \mathbf{a}_2 + \mathbf{b}_2^H \dot{\mathbf{b}}_2 \dot{\mathbf{a}}_2^H \mathbf{R}_X^* \mathbf{a}_2 \right) \end{bmatrix}. \tag{4.12}$$

By including prior information, the BFIM can be written as

$$\mathbf{J}_{\theta|\mathbf{X}} = \mathbf{F} + \mathbf{J}^P, \tag{4.13}$$

where, from (3.4), the prior Fisher information matrix is a matrix of  $2 \times 2$  matrices along its diagonal and zeroes everywhere else. The matrices along the diagonal express the prior information of the angles and the real and imaginary parts of the complex amplitudes, namely:

$$\mathbf{J}^P = \begin{bmatrix} \mathbf{J}_\theta^P & \mathbf{0} & \mathbf{0} \\ \mathbf{0} & \mathbf{J}_{\Re\{\beta\}}^P & \mathbf{0} \\ \mathbf{0} & \mathbf{0} & \mathbf{J}_{\Im\{\beta\}}^P \end{bmatrix}. \tag{4.14}$$

Since we are only interested in the estimation of the angles of arrival, we consider the equivalent Bayesian Fisher information matrix (BFIM) [1][12] by treating the complex amplitudes as nuisance parameters, namely,

$$\begin{aligned}
 \mathbf{J}_e(\boldsymbol{\theta}) = & 2\mathbb{E}_\beta \{ \mathbf{F}_{11} \} + \mathbf{J}_\theta^P \\
 & - 4\mathbb{E}_\beta \{ \mathbf{F}_{12}^* \} \left( 2\mathbb{E}_\beta \{ \mathbf{F}_{22} \} + \mathbf{J}_\beta^P \right)^{-1} \mathbb{E}_\beta \{ \mathbf{F}_{12} \}. \tag{4.15}
 \end{aligned}$$

We also work under the assumption that the complex amplitudes  $\beta_1, \beta_2$  are circularly symmetric, which implies that  $\mathbb{E}\{\beta_i\} = \mathbb{E}\{\beta_i^*\} = 0$ , and that  $J_{\Re\{\beta_i\}}^P = J_{\Im\{\beta_i\}}^P = J_{\beta_i}^P$  [1]. This also implies that  $\mathbb{E}_\beta \{ \mathbf{F}_{12}^* \} = \mathbb{E}_\beta \{ \mathbf{F}_{12} \} = \mathbf{0}$ .

We can thus focus on  $\mathbf{F}_{11}$  to obtain the CRB. We now introduce the assumption of uncorrelated complex coefficients, hence  $\mathbb{E}\{\beta_1 \beta_2\} = \mathbb{E}\{\beta_1\} \mathbb{E}\{\beta_2\}$ . When taking

the expected value (which is with respect to the nuisance parameter  $\boldsymbol{\beta}$ ), due to the circularly symmetric assumption of the complex amplitudes, we have the following:

$$\mathbb{E}_{\boldsymbol{\beta}} \left\{ \begin{bmatrix} \|\beta_1\|^2 & \beta_1^* \beta_2 \\ \beta_2^* \beta_1 & \|\beta_2\|^2 \end{bmatrix} \right\} = \begin{bmatrix} \mathbb{E}_{\beta_1} \{\|\beta_1\|^2\} & 0 \\ 0 & \mathbb{E}_{\beta_2} \{\|\beta_2\|^2\} \end{bmatrix}. \quad (4.16)$$

By choosing the phase reference point of the transmitting and receiving arrays such that  $\mathbf{b}_1^H \dot{\mathbf{b}}_1 = \dot{\mathbf{b}}_1^H \mathbf{b}_1 = \mathbf{b}_2^H \dot{\mathbf{b}}_2 = \dot{\mathbf{b}}_2^H \mathbf{b}_2 = 0$ , we arrive at:

$$\mathbb{E}\{\mathbf{F}_{11}\} = \frac{T}{\sigma_s^2} \begin{bmatrix} \mathbb{E}\{|\beta_1|^2\} f_1(\mathbf{R}_{\mathbf{X}}) & 0 \\ 0 & \mathbb{E}\{|\beta_2|^2\} f_2(\mathbf{R}_{\mathbf{X}}) \end{bmatrix} \quad (4.17)$$

where

$$f_i(\mathbf{R}_{\mathbf{X}}) := \mathbb{E}_{\theta_i} \{ \|\dot{\mathbf{b}}(\theta_i)\|^2 \text{tr} \{ \mathbf{a}(\theta_i) \mathbf{a}^H(\theta_i) \mathbf{R}_{\mathbf{X}}^* \} + \|\mathbf{b}(\theta_i)\|^2 \text{tr} \{ \dot{\mathbf{a}}(\theta_i) \dot{\mathbf{a}}^H(\theta_i) \mathbf{R}_{\mathbf{X}}^* \} \}. \quad (4.18)$$

An alternative way to express  $f_i(\mathbf{R}_{\mathbf{X}})$  is obtained by defining  $\bar{\mathbf{M}}_i = \mathbb{E}_{\theta_i} \{ \mathbf{M}^*(\theta_i) \}$ , with  $\mathbf{M}(\theta_i)$  being

$$\mathbf{M}(\theta_i) = \|\dot{\mathbf{b}}(\theta_i)\|^2 \mathbf{a}(\theta_i) \mathbf{a}^H(\theta_i) + \|\mathbf{b}(\theta_i)\|^2 \dot{\mathbf{a}}(\theta_i) \dot{\mathbf{a}}^H(\theta_i). \quad (4.19)$$

It is key to highlight that the matrix  $\mathbf{J}_{\boldsymbol{\theta}}^P$  defines the prior knowledge on the distribution of the angles  $\theta_1$  and  $\theta_2$ . Such matrix is assumed diagonal; hence, the priors of the angles are uncorrelated, with entries  $J_{\theta_1}^P$  and  $J_{\theta_2}^P$ . The two entries are the inverse of the known variances of the prior distribution for the two angles and can be either approximated using  $\sigma^2 \approx \frac{1}{\kappa}$  or by using the more accurate approximation  $\sigma^2 = 1 - \frac{I_1(\kappa)}{I_0(\kappa)}$ , where  $I_i(\kappa)$  is the modified Bessel function of order  $i$ .

It is possible to invert the resulting diagonal matrix and finally obtain:

$$\begin{aligned} \boldsymbol{\epsilon} = & \underbrace{\mathbb{E}_{\mathbf{X}} \left\{ \left( \frac{2T}{\sigma_s^2} \mathbb{E}_{\beta_1} \{|\beta_1|^2\} f_1(\mathbf{R}_{\mathbf{X}}) + J_{\theta_1}^P \right)^{-1} \right\}}_{\boldsymbol{\epsilon}_{\theta_1}} \\ & + \underbrace{\mathbb{E}_{\mathbf{X}} \left\{ \left( \frac{2T}{\sigma_s^2} \mathbb{E}_{\beta_2} \{|\beta_2|^2\} f_2(\mathbf{R}_{\mathbf{X}}) + J_{\theta_2}^P \right)^{-1} \right\}}_{\boldsymbol{\epsilon}_{\theta_2}}. \end{aligned} \quad (4.20)$$

The derived expression for  $\boldsymbol{\epsilon}$  is the sum of two errors: the estimation of  $\theta_1$  and  $\theta_2$ . We can keep this distinction and study how the rate changes in relation to these two errors. We also remark that the BCRB depends on the transmit signal  $\mathbf{X}$  through  $\mathbf{R}_{\mathbf{X}}$ .

We can rewrite the errors as follows:

$$\epsilon_{\theta_i} = \mathbb{E}_{\mathbf{X}} \left\{ \left( \frac{2T\mathbb{E}\{|\beta_i|^2\}}{\sigma^2} \text{tr}\{\bar{\mathbf{M}}_i \mathbf{R}_{\mathbf{X}}\} + J_{\theta_i}^P \right)^{-1} \right\}. \quad (4.21)$$

If we only focus on estimating the angle  $\theta_i$ , the optimal choice of  $\mathbf{R}_{\mathbf{X}}$  is known from previous work [1]. However, a closed form optimal solution for the joint estimation of multiple angles is not available. An optimal deterministic signal  $\mathbf{X}$  can be found numerically by using convex optimization tools such as CVX [14][15].

## 4.2 Optimal Communication and Sensing Points

In ISAC, we are trying to share resources between the sensing and communication tasks to optimize our transmission. Before diving into the proposed strategies, it is good to consider the optimal achievable points if the two tasks are not done jointly. Hence, here we study the deterministic optimal choice of  $\mathbf{X}$  that minimizes the total estimation error and the optimal  $\mathbf{X}$  that maximizes the ergodic rate. The goal is to find in the next chapter an achievable ISAC region that interpolates between these points.

### 4.2.1 Optimal Sensing Point

It is known [1] that to minimize the BCRB  $\epsilon_{\theta_i}$  of a single angle, hence falling back to the problem of single target estimation, we can achieve the optimal result by transmitting in the direction of the eigenvector corresponding to the largest eigenvalue of the matrix  $\bar{\mathbf{M}}_i$ .

However, finding an analytical solution is not as straightforward when investigating the joint minimization of both angles, which we have seen corresponds to minimizing the sum of the estimation error on each angle. It is left for future works to find a closed-term optimal solution for this problem, while for this dissertation to provide a reliable achievable point, we rely on a numerical optimization for any angle pair.

Since [1] provided the result that the rank of the optimal solution to this issue is equal to 2 and that by analyzing our resulting matrix  $\mathbf{R}_{\mathbf{X}}$  it has two main eigenvalues, we select the two main directions (the two eigenvectors corresponding to the two largest eigenvalues) of our numerical evaluation of the matrix  $\mathbf{R}_{\mathbf{X}}$ . We will refer to these two directions as  $\hat{\mathbf{r}}_{1,opt}$  and  $\hat{\mathbf{r}}_{2,opt}$ .

### 4.2.2 Optimal Communication Point

The optimal communications strategy for the communication-only point is obtained by solving

$$C = \max_{\mathbf{R}_X: \mathbb{E}\{\text{tr}\{\mathbf{R}_X\}\} \leq P_{\text{TX}}M_{\text{TX}}} R; \quad (4.22)$$

$$R := \mathbb{E}_{\mathbf{H}_c} \left[ \log_2 \left| I + \frac{1}{\sigma_e^2} \mathbf{H}_c^H \mathbb{E}_X[\mathbf{R}_X] \mathbf{H}_c \right| \right] = \mathbb{E}_{\alpha, \theta_c} \left[ \log \left( 1 + \frac{|\alpha|^2}{\sigma_e^2} \mathbf{a}^H(\theta_c) \mathbb{E}_X[\mathbf{R}_X] \mathbf{a}(\theta_c) \right) \right]; \quad (4.23)$$

which is again solvable with a numerical optimizer such as CVX.

Our simulations consider a LoS channel with a single receiver antenna; hence, the channel can be written as  $\mathbf{h}_c$ . If we consider the uncertainty on  $\mathbf{h}_c$  small, the optimal solution is simply to transmit Gaussian information alongside the direction that is the hermitian of the channel. We will refer to this direction as  $\hat{\mathbf{r}}_{c, \text{opt}}$ .

### 4.3 Ways to Characterize the ISAC Region

In this dissertation, we have studied the optimal sensing and communication points, practically providing an outer bound for the BCRB-Rate region, and are now interested in characterizing an inner bound. This problem can be solved in different ways:

1. Evaluation of parameterized achievable scheme and computation of the convex closure of achievable pair  $(R, \epsilon)$ .
2. Solve the constrained optimization problem:

$$\max_{p_{\mathbf{X}}(\mathbf{X}) \in \mathcal{X}(P_{\text{TX}}M_{\text{TX}})} I(\mathbf{X}; \mathbf{Y}_c | \mathbf{H}_c) \quad \text{s.t. } \epsilon = \epsilon_{\theta_1} + \epsilon_{\theta_2} \leq \epsilon_{\text{fix}}, \quad \forall \epsilon_{\text{fix}} \in [\epsilon_{\min}, 1], \quad (4.24)$$

where  $\mathcal{X}(P_{\text{TX}}M_{\text{TX}})$  is the set of all possible distributions for the input signal that meet the average power constraint  $P_{\text{TX}}M_{\text{TX}}$ , i.e.,  $\mathbb{E}\{\text{tr}\{\mathbf{R}_X\}\} \leq P_{\text{TX}}M_{\text{TX}} = P_{\text{TX}}M_{\text{TX}}$ ; and  $\epsilon_{\min}$  is the error obtained with (4.20) by using the  $\mathbf{R}_X$  obtained via CVX as described in section 4.2.1.

3. Solve the constrained optimization problem:

$$\min_{p_{\mathbf{X}}(\mathbf{X}) \in \mathcal{X}(P_{\text{TX}}M_{\text{TX}})} \epsilon \quad \text{s.t. } I(\mathbf{X}; \mathbf{Y}_c | \mathbf{H}_c) \leq R_{\text{fix}}, \quad \forall R_{\text{fix}} \in [0, R_{\max}], \quad (4.25)$$

where  $R_{\max} = \max_{p_{\mathbf{X}}(\mathbf{X}) \in \mathcal{X}(P_{\text{TX}}M_{\text{TX}})} I(\mathbf{X}; \mathbf{Y}_c | \mathbf{H}_c)$ .

4. Solve the constrained optimization problem:

$$\max_{p_{\mathbf{X}}(\mathbf{X}) \in \mathcal{X}(P_{\text{TX}}M_{\text{TX}})} \left\{ I(\mathbf{X}; \mathbf{Y}_c | \mathbf{H}_c) - \zeta \epsilon \right\}, \quad (4.26)$$

where  $\mathcal{X}(P_{\text{TX}}M_{\text{TX}})$  is the set of all possible distributions for the input signal that meet the average power constraint  $P_{\text{TX}}M_{\text{TX}}$ , i.e.,  $\mathbb{E}\{\text{tr}\{\mathbf{R}_X\}\} \leq P_{\text{TX}}M_{\text{TX}}$ ,

and the parameter  $\zeta \in [0, +\infty)$  is making it possible to optimize the curve so that for any given value of the rate the lowest error on the joint estimation of the angles is achieved, and that for any given value of  $\epsilon$  the maximum rate is achieved.

However, only the first way to solve the problem provides clear interpretability of the results regarding the optimal transmission strategy. For this reason, we focus on the first one in the next chapter.

## Chapter 5

# Achievable Transmission Strategies for Characterization of ISAC Tradeoff

### 5.1 General Communicating Strategy to the UE

We transmit a signal  $\mathbf{X}$  that needs to be optimized to obtain the lowest possible estimation error on the angles and the highest possible communication rate. In the signal  $\mathbf{X}$ , we must decide the direction(s) we want to send the signal and how we want to deliver information.

The next sections will apply different strategies to study the ISAC tradeoff. All of the strategies proposed in this work can be written in a general way as follows:

$$\mathbf{X} = [\mathbf{X}_1, \dots, \mathbf{X}_T] : \mathbf{X}_t = \sum_{b=1}^{N_B} \sqrt{P_{s;b,t}} \mathbf{s}_{b,t} + \sqrt{P_{c;b,t}} \mathbf{c}_{b,t} G_{b,t}, \quad (5.1)$$

where  $N_B$  is the number of beams one wishes to use,  $\mathbf{s}_{b,t}$  is a deterministic vector for sensing of unit length, and  $\mathbf{c}_{b,t}$  is a communication-beamforming vector which is normalized and ‘modulated’ by the information-carrying i.i.d.  $\mathcal{N}(0,1)$  Gaussian random variable  $G_{b,t}$ . The signal  $\mathbf{X}$  is subject to the power constraint  $\sum_{b=1}^{N_B} P_{s;b,t} + P_{c;b,t} \leq P_{\text{TX}} M_{\text{TX}}$ , which ensures that  $\mathbb{E}[\text{tr}\{\mathbf{R}_{\mathbf{X}}\}] \leq P_{\text{TX}} M_{\text{TX}}$ .

We will analyze specific choices of the various parameters on the proposed ISAC scheme, with specific channel parameters, to provide some case studies. We will use for each proposed strategy different choices for the directions of sensing and

communication. Those directions will be spanned through selection of parameters  $\lambda_i$ , such that  $\sum_i \lambda_i \leq 1$  and each  $\lambda_i \in [0, 1]$ .

### 5.1.1 Communication Rate for Given Strategy

It is equally important in this study to evaluate the rate for any given structure of the signal we want to transmit. Based on the generic transmitted signal in (5.1), we can compute the rate as:

$$R(\epsilon_{fix}) = \mathbb{E}_{\mathbf{h}_c} \left[ \sum_{t=1}^T \log \left( 1 + \frac{1}{T\sigma_c^2} \left( \sum_{b=1}^{N_B} P_{c;b,t} |\mathbf{h}_c^H \mathbf{c}_{b,t}|^2 \right) \right) \right]. \quad (5.2)$$

### 5.1.2 BCRB for Given Strategy

To compute the BCRB for the given strategy, we take the transmitted signal  $\mathbf{X}$  and directly apply:

$$\epsilon = \epsilon_{\theta_1} + \epsilon_{\theta_2}, \quad (5.3)$$

where:

$$\epsilon_{\theta_i} = \mathbb{E}_{\mathbf{X}} \left\{ \left( \frac{2T\mathbb{E}\{|\beta|^2\}}{\sigma^2} \text{tr}\{\bar{\mathbf{M}}_i \mathbf{R}_{\mathbf{X}}\} + J_{\theta_i}^P \right)^{-1} \right\}. \quad (5.4)$$

Note that we refer to  $\theta_1$  as the angle of the sensing only target and to  $\theta_2$  as the angle of the communication target to send data to and to sense at the same time.

## 5.2 Strategy 1: One Information Carrying Beam

For the first strategy, we send only in the direction we send i.i.d. Gaussian random variables, hence  $P_{s,t} = 0$ . We also transmit in the same direction for all  $t \in [1, T]$ . The transmit signal is then:

$$\mathbf{X} = [\mathbf{X}_1, \dots, \mathbf{X}_T] : \mathbf{X}_t = \sqrt{P_{\text{TX}} M_{\text{TX}}} \mathbf{c}_{\text{first}} G_t. \quad (5.5)$$

For this strategy, a closed form solution of (4.21) is derived in [1]:

$$\epsilon_{\theta_i, \text{first}} = \left( 2(T-1) \text{SNR}_s \mathbf{c}_{\text{first}}^H \bar{\mathbf{M}}_i \mathbf{c}_{\text{first}} \right)^{-1} (1 + r_\zeta), \quad (5.6)$$

where  $\text{SNR}_s = M_{\text{TX}} P_{\text{TX}} \mathbb{E}\{|\beta|^2\} \sigma_s^{-2}$ . The correction term  $r_\zeta$  is given by

$$r_\zeta = \sum_{n=1}^{T-2} \frac{(-1)^n \zeta^n}{\prod_{i=1}^n (T-i-1)} + \underbrace{(-1)^{T-1} \cdot \frac{e^\zeta \zeta^{T-1} \Gamma(0, \zeta)}{\Gamma(T-1)}}_{O(\zeta^{T-1} \log \zeta)}, \quad (5.7)$$



where  $\Gamma(a, x) = \int_x^\infty t^{a-1} e^{-t} dt$ , denotes the incomplete Gamma function, and the variable  $\zeta$  is computed as  $\zeta = J_{\theta_i}^P \left( 2 \text{SNR}_s \mathbf{c}_{\text{first}}^H \bar{\mathbf{M}} \mathbf{c}_{\text{first}} \right)^{-1}$ .

For what concerns the communication rate, this strategy yields:

$$R = \mathbb{E}_{\mathbf{h}_c} \left[ \log_2 \left( 1 + \mathbb{E}_{\mathbf{h}_c} [\|\mathbf{h}_c\|^2]^{-1} |\mathbf{c}_{\text{first}}^H \mathbf{h}_c|^2 \text{SNR}_c \right) \right], \quad (5.8)$$

where  $\text{SNR}_c = M_{\text{TX}} P_{\text{TX}} \mathbb{E}_{\mathbf{h}_c} [\|\mathbf{h}_c\|^2] \sigma_c^{-2}$ .

### 5.2.1 Choice 1: Spanning among the two main eigenvectors of $\bar{\mathbf{M}}_1$ , and the two main eigenvectors of $\bar{\mathbf{M}}_2$

For the direction  $\mathbf{c}_{\text{first}}$ , we start by spanning between the two eigenvectors corresponding to the largest eigenvalues of the matrices  $\bar{\mathbf{M}}_1$  and  $\bar{\mathbf{M}}_2$ . The choice is motivated by the fact that the error on the estimation of each angle is minimized by choosing as direction the “main” eigenvector corresponding to the largest eigenvalue of the corresponding  $\bar{\mathbf{M}}_i$  matrix [1], and since if the angle distribution is very narrow the rank of the matrices is 2, by choosing the two main directions we try to see if for the case of joint target angles estimation, using a direction different than the main one can help. Denoting by  $\mathbf{v}_1$  and  $\mathbf{v}_2$  the two main eigenvectors of  $\bar{\mathbf{M}}_1$ , and as  $\mathbf{v}_3$  and  $\mathbf{v}_4$  the ones of  $\bar{\mathbf{M}}_2$ , we can write the direction of transmission as:

$$\mathbf{r} = \sqrt{\lambda_1} \mathbf{v}_1 + \sqrt{\lambda_2} \mathbf{v}_2 + \sqrt{\lambda_3} \mathbf{v}_3 + \sqrt{\lambda_4} \mathbf{v}_4, \quad \mathbf{c}_{\text{first}} = \frac{\mathbf{r}}{\|\mathbf{r}\|}. \quad (5.9)$$

### 5.2.2 Choice 2: Spanning among the Directions of the Optimal Sensing and the Direction of Optimal Communication

Another strategy is to span between the two optimal directions obtained via CVX for the overall minimization of the BCRB and the optimal direction of communication. We construct our direction of transmission as follows:

$$\mathbf{r} = \sqrt{\lambda_1} \hat{\mathbf{r}}_{1,\text{opt}} + \sqrt{\lambda_2} \hat{\mathbf{r}}_{2,\text{opt}} + \sqrt{\lambda_3} \hat{\mathbf{r}}_{c,\text{opt}} \quad \mathbf{c}_{\text{first}} = \frac{\mathbf{r}}{\|\mathbf{r}\|}. \quad (5.10)$$

## 5.3 Strategy 2: One Information-less Beam

For the second strategy, we send only in the direction without Gaussian random variables, hence  $P_{c,t} = 0$ . We also transmit in the same direction for all  $t \in [1, T]$ . The transmit signal is then:

$$\mathbf{X} = [\mathbf{X}_1, \dots, \mathbf{X}_T] : \mathbf{X}_t = \sqrt{P_{\text{TX}} M_{\text{TX}}} \mathbf{s}_{\text{second}}. \quad (5.11)$$

For this strategy, a closed form solution of 4.21 is derived in [1]:

$$\epsilon_{\theta_i, \text{second}} = \left( 2T \text{SNR}_s \mathbf{s}_{\text{second}}^H \overline{\mathbf{M}}_i \mathbf{s}_{\text{second}} + J_{\theta_i}^P \right)^{-1}. \quad (5.12)$$

Due to the lack of information, the resulting rate will be zero. Given that this strategy returns a zero rate, it is presented to provide some insights into the minimum values for the joint estimation of the two angles.

### 5.3.1 Choice 1: Spanning among the two main eigenvectors of $\overline{\mathbf{M}}_1$ , and the two main eigenvectors of $\overline{\mathbf{M}}_2$

The first spanning choice uses the same direction as the first direction choice in 5.2.1 to compare them. Hence, the direction is chosen as follows:

$$\mathbf{r} = \sqrt{\lambda_1} \mathbf{v}_1 + \sqrt{\lambda_2} \mathbf{v}_2 + \sqrt{\lambda_3} \mathbf{v}_3 + \sqrt{\lambda_4} \mathbf{v}_4, \quad \mathbf{s}_{\text{second}} = \frac{\mathbf{r}}{\|\mathbf{r}\|}. \quad (5.13)$$

### 5.3.2 Choice 2: Spanning among the main eigenvector of $\overline{\mathbf{M}}_1$ , the main eigenvector of $\overline{\mathbf{M}}_2$ and the Directions of Optimal Sensing

The second choice uses the main components of the  $\overline{\mathbf{M}}_i$  matrices and the optimal directions for minimizing the BCRB obtained via CVX. The direction is then chosen as follows:

$$\mathbf{r} = \sqrt{\lambda_1} \hat{\mathbf{r}}_{1, \text{opt}} + \sqrt{\lambda_2} \hat{\mathbf{r}}_{2, \text{opt}} + \sqrt{\lambda_3} \mathbf{v}_1 + \sqrt{\lambda_4} \mathbf{v}_3 \quad \mathbf{s}_{\text{second}} = \frac{\mathbf{r}}{\|\mathbf{r}\|}. \quad (5.14)$$

## 5.4 Strategy 3: Both One Information Carrying Beam and One Information-less Beam

For the third strategy, we send in both the directions highlighted in the general transmission signal (5.1). We transmit in the same directions or all  $t \in [1, T]$ . The transmit signal is then:

$$\mathbf{X} = [\mathbf{X}_1, \dots, \mathbf{X}_T] : \mathbf{X}_t = \sqrt{P_s} \mathbf{s}_{\text{third}} + \sqrt{P_c} \mathbf{c}_{\text{third}} G_t. \quad (5.15)$$

Note that power allocation becomes a key factor for this strategy. When spanning among different directions we will also be affecting the power allocation towards  $P_s$  and  $P_c$ , respectively.

For what concerns the communication rate, this strategy yields:

$$R = \mathbb{E}_{\mathbf{h}_c} \left[ \log_2 \left( 1 + \mathbb{E}_{\mathbf{h}_c} [\|\mathbf{h}_c\|^2]^{-1} \left| \mathbf{c}_{\text{third}}^H(\lambda) \mathbf{h}_c \right|^2 \text{SNR}_c \right) \right], \quad (5.16)$$

where  $\text{SNR}_c = P_c \mathbb{E}_{\mathbf{h}_c} [\|\mathbf{h}_c\|^2] \sigma_c^{-2}$ . We will express  $P_c$  as a function of the maximum power  $P_{\text{TX}} M_{\text{TX}}$  based on the directions used.

#### 5.4.1 Choice 1: Spanning among the main eigenvector of $\bar{\mathbf{M}}_1$ , the main eigenvector of $\bar{\mathbf{M}}_2$ and the Direction of Optimal Communication

As a first choice, we use for the sensing direction  $\mathbf{s}$  the main eigenvector corresponding to the largest eigenvalue of  $\bar{\mathbf{M}}_1$  and  $\bar{\mathbf{M}}_2$ , which are  $\mathbf{v}_1$  and  $\mathbf{v}_3$  respectively. The optimal communication direction  $\hat{\mathbf{r}}_{c,opt}$  is used for the communication direction  $\mathbf{c}$ . We can write the directions as:

$$\mathbf{r}_1 = \sqrt{\lambda_1} \mathbf{v}_1 + \sqrt{\lambda_2} \mathbf{v}_3, \quad \mathbf{s}_{\text{third}} = \frac{\mathbf{r}_1}{\|\mathbf{r}_1\|}, \quad (5.17)$$

$$\mathbf{r}_2 = \sqrt{\lambda_3} \hat{\mathbf{r}}_{c,opt}, \quad \mathbf{c}_{\text{third}} = \frac{\mathbf{r}_2}{\|\mathbf{r}_2\|}. \quad (5.18)$$

The spanning choice allows us to compute the power devoted to the sensing-focused direction  $P_s$  and communication-focused direction as  $P_s = (\lambda_1 + \lambda_2) P_{\text{TX}} M_{\text{TX}}$  and  $P_c = \lambda_3 P_{\text{TX}} M_{\text{TX}}$ , respectively.

#### 5.4.2 Choice 2: Spanning among the Directions of the Optimal Sensing and the Direction of Optimal Communication

As a second choice, we choose the sensing direction  $\mathbf{s}$  to span between the two optimal directions for sensing obtained via CVX. For the communication side, we utilize instead the optimal direction  $\hat{\mathbf{r}}_{c,opt}$ . We can write the directions as follows:

$$\mathbf{r}_1 = \sqrt{\lambda_1} \hat{\mathbf{r}}_{1,opt} + \sqrt{\lambda_2} \hat{\mathbf{r}}_{2,opt}, \quad \mathbf{s}_{\text{third}} = \frac{\mathbf{r}_1}{\|\mathbf{r}_1\|}, \quad (5.19)$$

$$\mathbf{r}_2 = \sqrt{\lambda_3} \hat{\mathbf{r}}_{c,opt}, \quad \mathbf{c}_{\text{third}} = \frac{\mathbf{r}_2}{\|\mathbf{r}_2\|}. \quad (5.20)$$

The spanning choice allows us to compute the power devoted to the sensing-focused direction  $P_s$  and communication-focused direction as  $P_s = (\lambda_1 + \lambda_2) P_{\text{TX}} M_{\text{TX}}$  and  $P_c = \lambda_3 P_{\text{TX}} M_{\text{TX}}$ , respectively.

### 5.4.3 Choice 3: Spanning among the main eigenvector of $\bar{\mathbf{M}}_1$ , the main eigenvector of $\bar{\mathbf{M}}_2$ , the Directions of the Optimal Sensing, and the Direction of Optimal Communication

As a third and final choice we use a combination of the previous choices in 5.4.1 and 5.4.2. For the sensing-focused direction  $\mathbf{s}$ , we use a combination of both the main eigenvector corresponding to the largest eigenvalue of  $\bar{\mathbf{M}}_1$  and  $\bar{\mathbf{M}}_2$ , and also the two optimal directions for sensing obtained via CVX. For the communication-focused direction, we use optimal communication direction  $\hat{\mathbf{r}}_{c,opt}$ . We can write the directions as follows:

$$\mathbf{r}_1 = \sqrt{\lambda_1}\mathbf{v}_1 + \sqrt{\lambda_2}\mathbf{v}_3 + \sqrt{\lambda_3}\hat{\mathbf{r}}_{1,opt} + \sqrt{\lambda_4}\hat{\mathbf{r}}_{2,opt}, \quad \mathbf{s}_{\text{third}} = \frac{\mathbf{r}_1}{\|\mathbf{r}_1\|}, \quad (5.21)$$

$$\mathbf{r}_2 = \sqrt{\lambda_5}\hat{\mathbf{r}}_{c,opt}, \quad \mathbf{c}_{\text{third}} = \frac{\mathbf{r}_2}{\|\mathbf{r}_2\|}. \quad (5.22)$$

The spanning choice allows us to compute the power devoted to the sensing-focused direction  $P_s$  and communication-focused direction as  $P_s = (\lambda_1 + \lambda_2 + \lambda_3 + \lambda_4)P_{\text{TX}}M_{\text{TX}}$  and  $P_c = \lambda_5P_{\text{TX}}M_{\text{TX}}$ , respectively.

# Chapter 6

## Simulation Results

In this chapter, we provide different simulations for each of the strategies and choices of direction presented in the previous chapter.

We start with a batch of simulations sharing the same parameters specified in 6.1 to be able to compare them effectively. Note that we assume colocated TX and RX antennas; hence, the spacing and number of antennas are the same.

**Table 6.1:** Parameters Used to Compare Different Strategies

Configuration	Value
No. antennas ( $M_{TX} = M_{RX}$ )	10
Antennas spacing	1/2 wavelength
Max. Sensing Receiving SNR	20dB per Antenna
Max. Communication Receiving SNR	33dB per Antenna
Coherence Time ( $T$ )	3
Mean Sensing Angle ( $\theta_s$ )	30°
Concentration of Sensing Angle ( $\kappa$ )	131.8
Mean Communication Angle ( $\theta_c$ )	42°
Concentration of Communication Angle ( $\kappa$ )	131.8
Number of Simulated Sensing Angles	10,000
Number of Simulated Communication Angles	1,000
Number of Simulated Gaussians	10,000

Since the theoretical formulas for the first strategy are available, the theoretical plots are provided and compared with the simulated results. The presented plots can either represent the total BCRB, given by the sum of the ones on each angle, against the rate or the relationship between each BCRB on the x and y axes, respectively, with the rate represented through colors. Since the total rate is zero for the second transmission strategy, representing the total error vs. the rate does

not provide insights.

## 6.1 Strategy 1: One Information Carrying Beam

### 6.1.1 Choice 1: Spanning among the two main eigenvectors of $\bar{\mathbf{M}}_1$ , and the two main eigenvectors of $\bar{\mathbf{M}}_2$

The results shown in 6.1 confirm the validity of our simulation compared to the theoretical results in 6.2. It is possible to appreciate how, by using the eigenvectors of the matrices  $\bar{\mathbf{M}}_1$  and  $\bar{\mathbf{M}}_2$ , it is possible to achieve the lowest errors on the single angle estimation. However, it is in our interest to study the joint estimation; hence, having more points in the low-left corner of both figures would be desirable. It is also important to highlight that using this strategy, it is possible to achieve optimal communication rates, as confirmed by the results in 6.3 and 6.4. However, the choice of this strategy does not allow us to reach the minimum overall achievable error on the estimation, which requires a deterministic signal. This can be confirmed by the result in 6.5, in which the outer bound of the scatter plot in 6.4 is taken. It is possible to appreciate the difference between the overall minimum achievable error and the one we can achieve with the first strategy. Note how there is a gap between the total error we obtain with this choice of direction and the minimum achievable error for the first strategy. This is because, as mentioned, there is a lack of points that produce low errors on both the estimation of  $\theta_1$  and  $\theta_2$ .

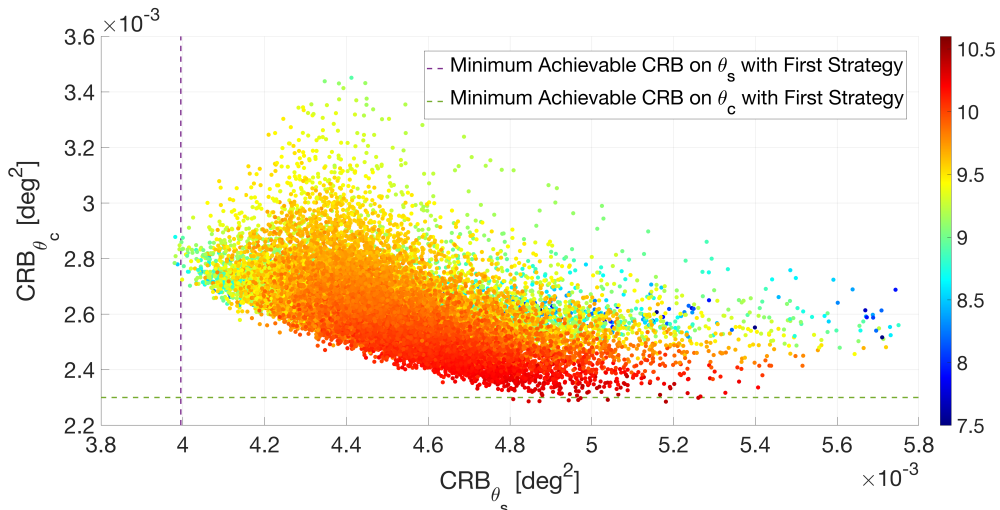
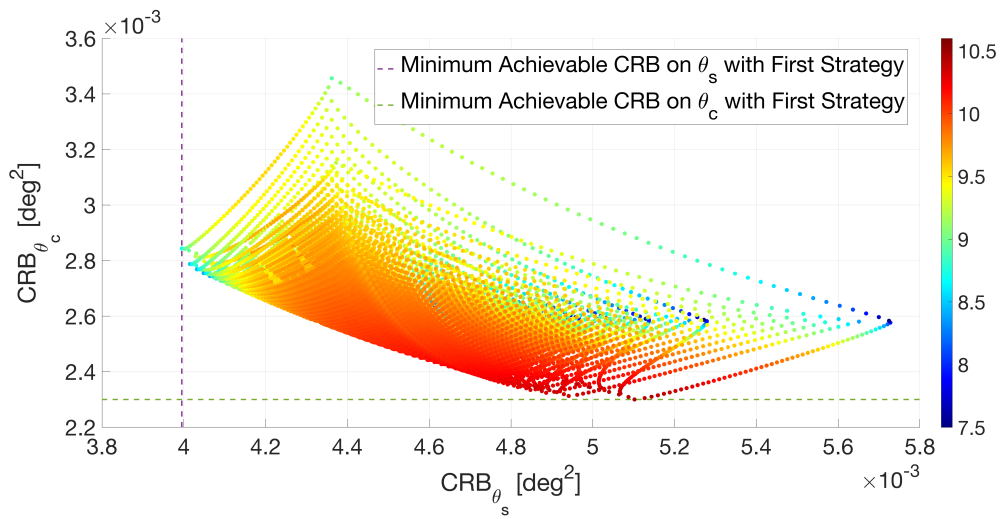
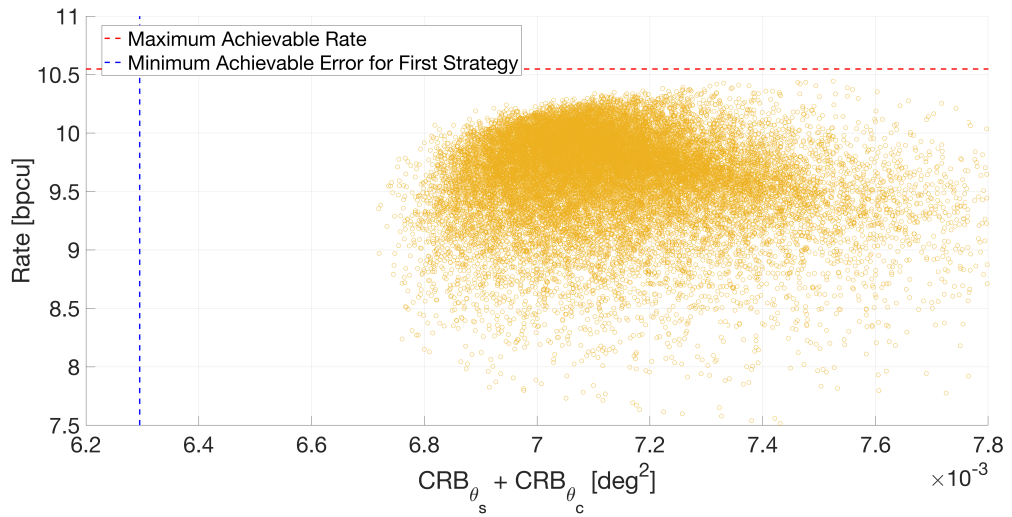


Figure 6.1: First Strategy, First Direction Choice, BCRB-Rate Simulated Points.



**Figure 6.2:** First Strategy, First Direction Choice, BCRB-Rate Theoretical Points.



**Figure 6.3:** First Strategy, First Direction Choice, Total BCRB-Rate Simulated Points.

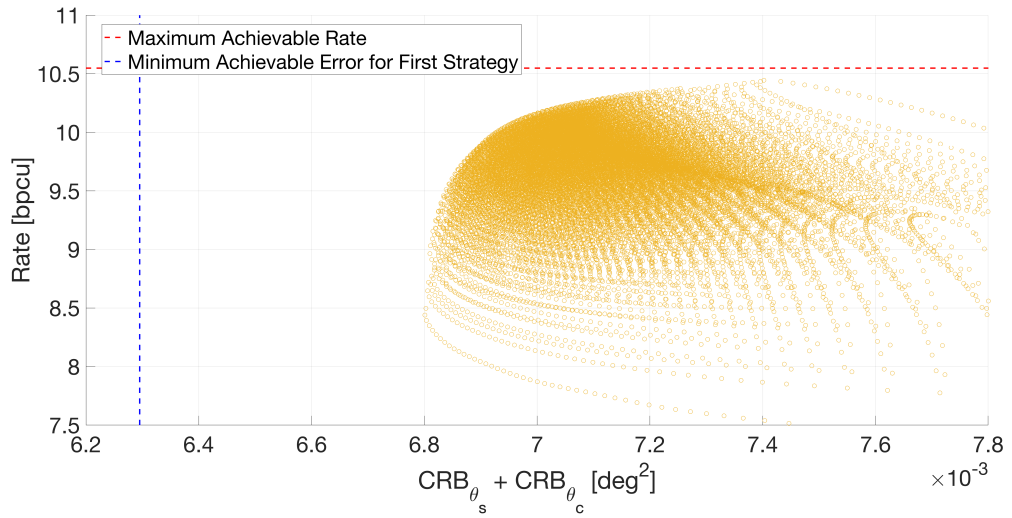


**Figure 6.4:** First Strategy, First Direction Choice, Total BCRB-Rate Theoretical Points.

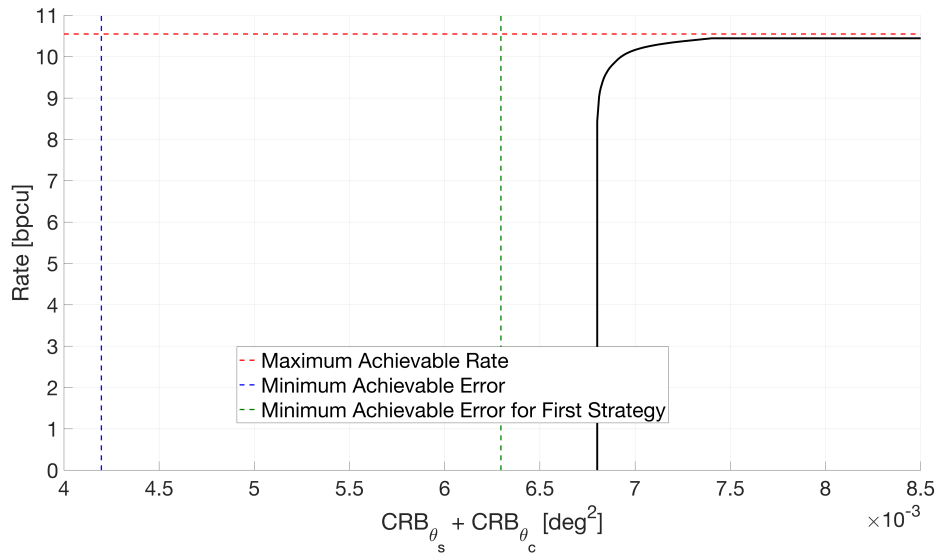


**Figure 6.5:** First Strategy, First Direction Choice, Total BCRB-Rate Outer Bound.



### 6.1.2 Choice 2: Spanning among the Directions of the Optimal Sensing and the Direction of Optimal Communication

We mentioned the importance of having points in the low-left of the figures representing the CRB of each angle in the x and y-axis, respectively. This is possible using the directions obtained via CVX, as seen in 6.6 and 6.7. As expected, as a consequence of this, it is also able to achieve a lower total error than the previous choice, as it can be seen in 6.8 and 6.9. The comparison is even more appreciable in 6.11, where the choices for this strategy are compared.

Overall, from this first strategy, we could say that using the eigenvectors of the matrices  $\bar{\mathbf{M}}_1$  and  $\bar{\mathbf{M}}_2$  is more suitable if interested in one specific angle. Using a more optimal solution for the joint estimation is certainly more suitable for the overall minimization of the total error.

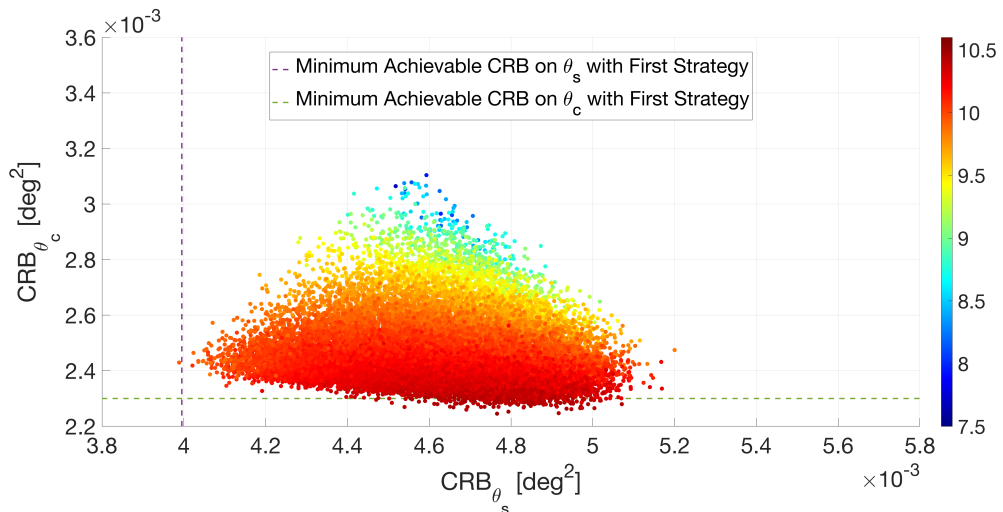


**Figure 6.6:** First Strategy, Second Direction Choice, BCRB-Rate Simulated Points.

## 6.2 Strategy 2: One Information-less Beam

### 6.2.1 Choice 1: Spanning among the two main eigenvectors of $\bar{\mathbf{M}}_1$ , and the two main eigenvectors of $\bar{\mathbf{M}}_2$

The second strategy, returning a zero rate, focuses on the sensing side of our study. Since we are now sending a deterministic signal, achieving the optimal estimation errors is possible. In particular, with this first choice of direction, it can be seen

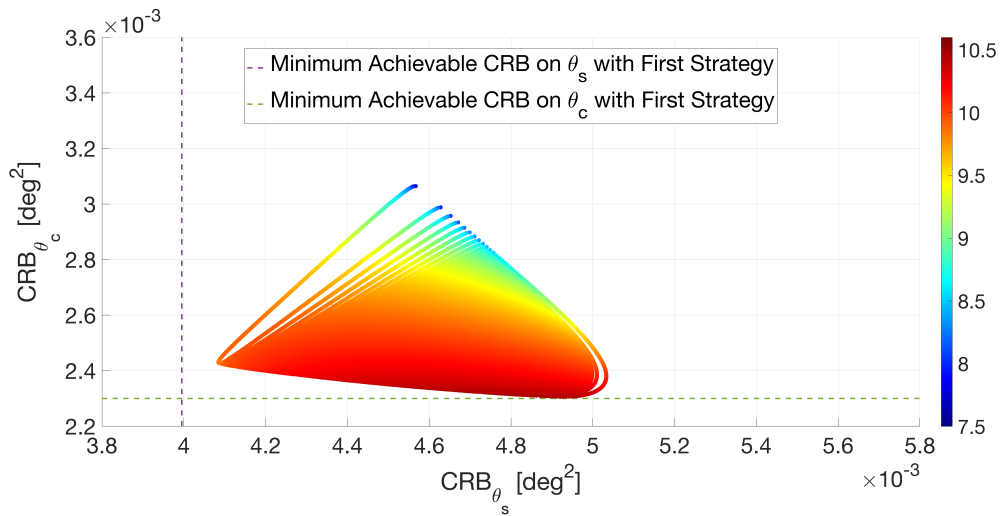


**Figure 6.7:** First Strategy, Second Direction Choice, BCRB-Rate Theoretical Points.

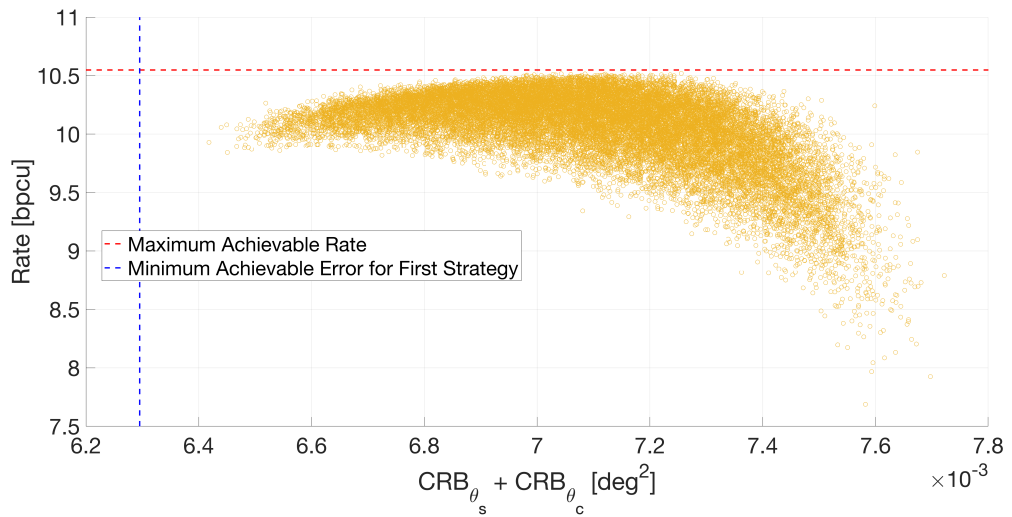


**Figure 6.8:** First Strategy, Second Direction Choice, Total BCRB-Rate Simulated Points.

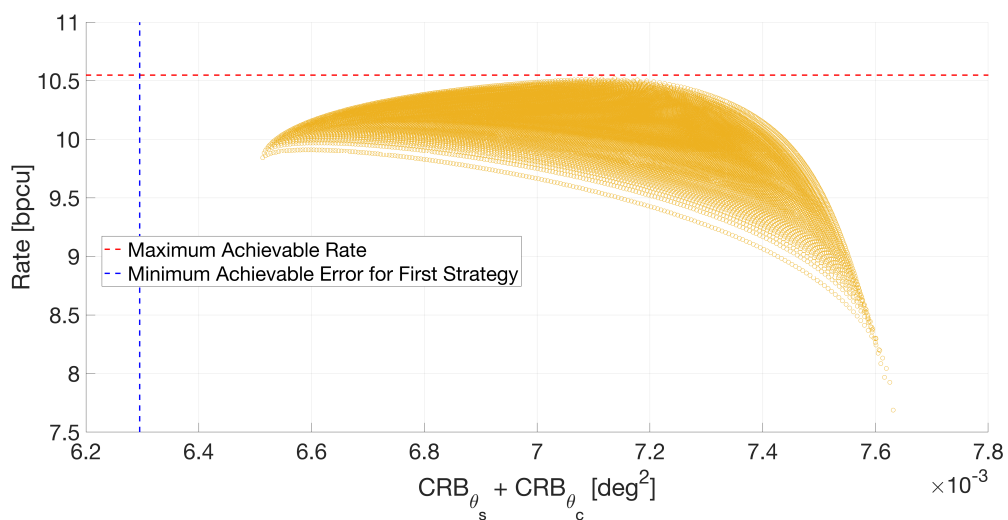


**Figure 6.9:** First Strategy, Second Direction Choice, Total BCRB-Rate Theoretical Points.

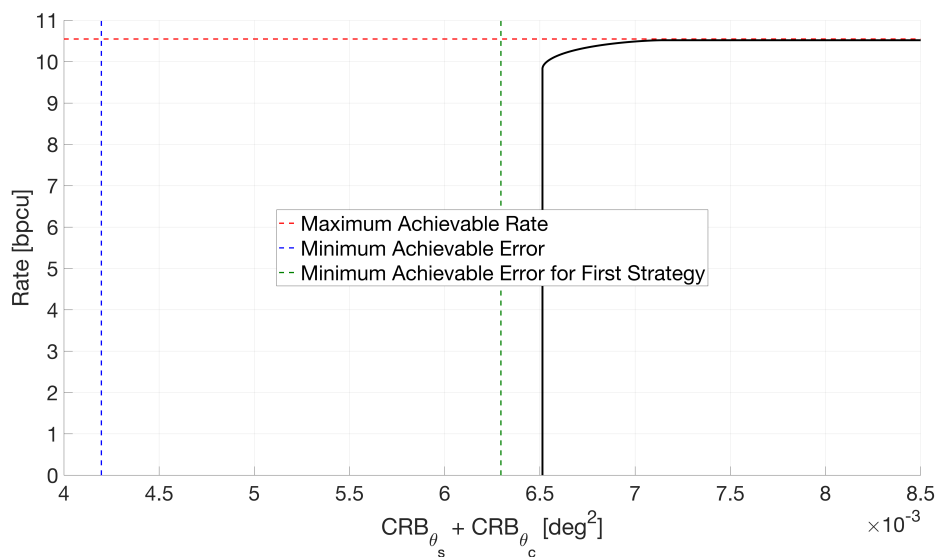


**Figure 6.10:** First Strategy, Second Direction Choice, Total BCRB-Rate Outer Bound.

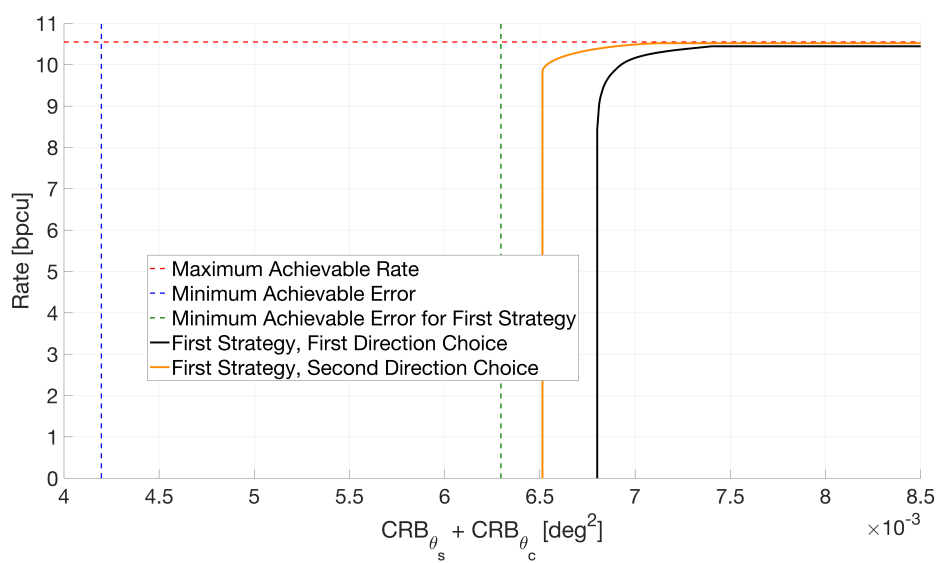


**Figure 6.11:** First Strategy, Comparison of Direction Choice, Total BCRB-Rate Outer Bound.

in 6.12 that by using the eigenvectors of  $\overline{\mathbf{M}}_1$  and  $\overline{\mathbf{M}}_2$  it is possible to reach the optimal values for the estimation of each of the angles by themselves. However, as in the previous strategy, having points in the low-left region would be desirable if focusing on minimizing the joint estimation of the angles.

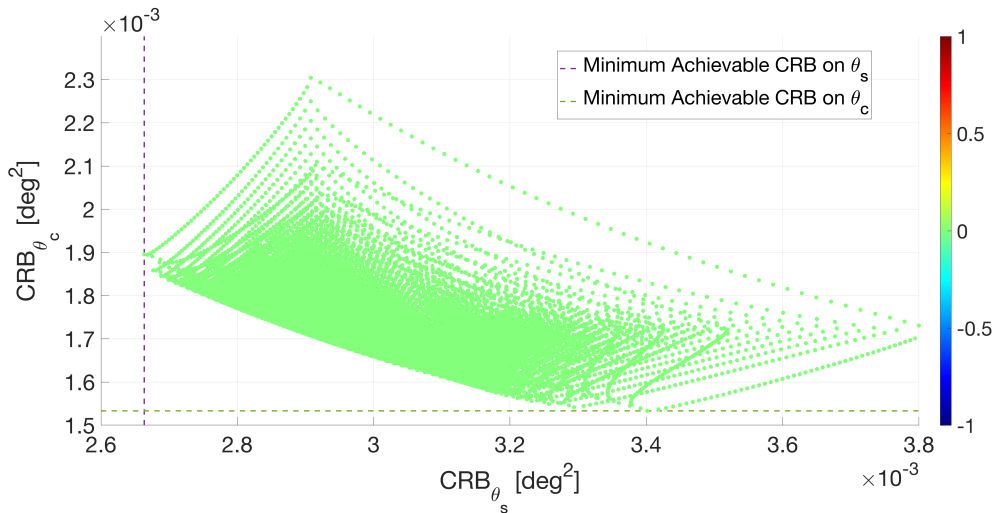


**Figure 6.12:** Second Strategy, First Direction Choice, BCRB-Rate Simulated Points.

### 6.2.2 Choice 2: Spanning among the main eigenvector of $\overline{\mathbf{M}}_1$ , the main eigenvector of $\overline{\mathbf{M}}_2$ and the Directions of Optimal Sensing

As per the results for the previous strategy, it is possible to see in this scenario as well how by using the optimal directions found via CVX, it is possible to fill the plot's lower-left portion in 6.13.

In this case, since we are also spanning among the eigenvectors of  $\overline{\mathbf{M}}_1$ , we reach the minimum estimation error for  $\theta_1$ , which was not reached in 6.7 as we were spanning on the optimal directions or the joint sensing only.

### 6.3 Strategy 3: Both One Information Carrying Beam and One Information-less Beam

This strategy combines the things we could notice from the previous two. Without sending Gaussian i.i.d. random variables (information-less beam), we can achieve

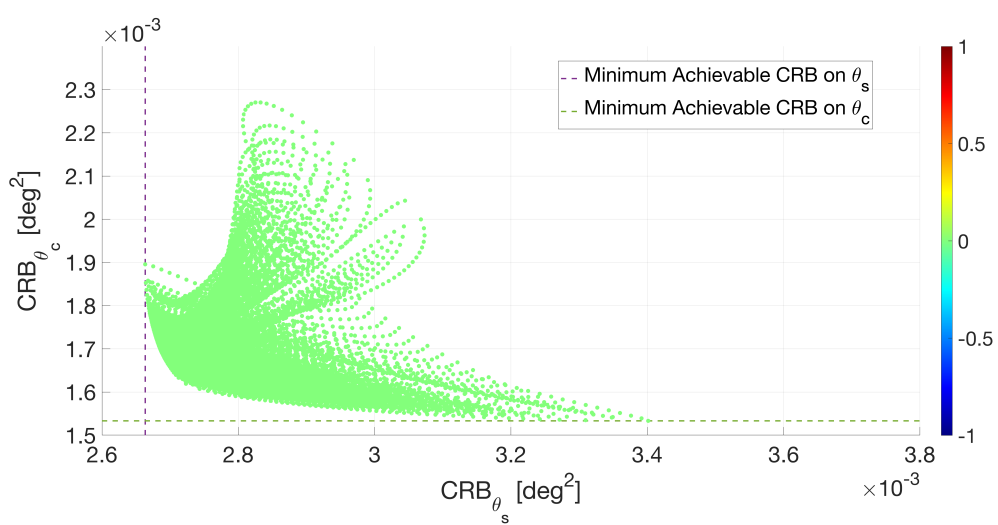


**Figure 6.13:** Second Strategy, Second Direction Choice, BCRB-Rate Simulated Points.

the minimum BCRB point, while we need the information carrying beam to achieve the highest possible rate.

### 6.3.1 Choice 1: Spanning among the main eigenvector of $\bar{\mathbf{M}}_1$ , the main eigenvector of $\bar{\mathbf{M}}_2$ and the Direction of Optimal Communication

As expected, in 6.14, we can see that by using the eigenvectors of  $\bar{\mathbf{M}}_1$  and  $\bar{\mathbf{M}}_2$ , we can achieve the lowest error on the single angle estimation of  $\theta_1$  or  $\theta_2$ . Using this strategy, we can span between points that optimize the single angle estimation and points that optimize the communication rate. This could provide a valid strategy for using ISAC in this two-angle scenario by using proper power allocation between the beams if interested in minimizing the single-angle estimation error.

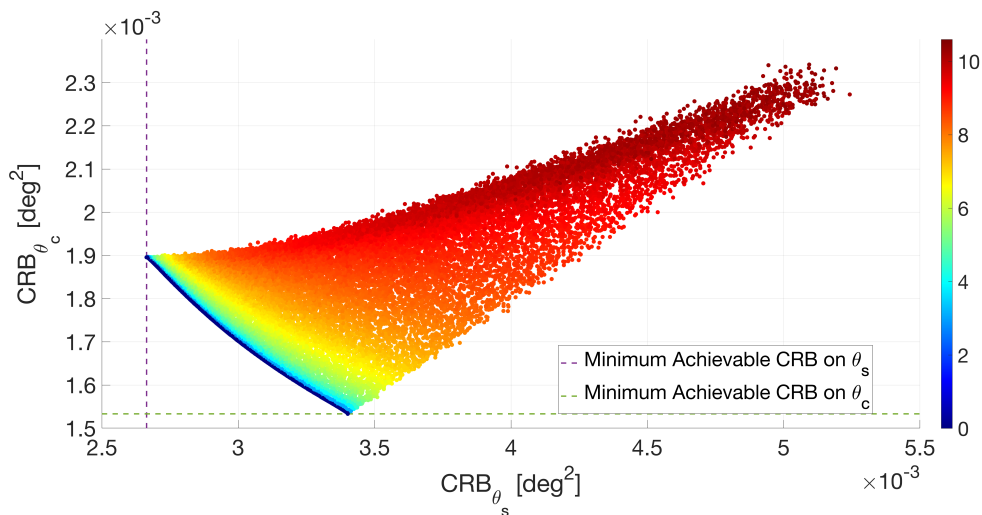


**Figure 6.14:** Third Strategy, First Direction Choice, BCRB-Rate Simulated Points.

### 6.3.2 Choice 2: Spanning among the Directions of the Optimal Sensing and the Direction of Optimal Communication

Using the optimal directions for the joint estimation, it is possible to have more points in the low-left region in 6.17 compared to the previous choice (in 6.14). This leads to an overall lower error when considering the joint estimation of the angles as in 6.18. However, we again highlight that the minimum points for the single angle estimations have not been reached.

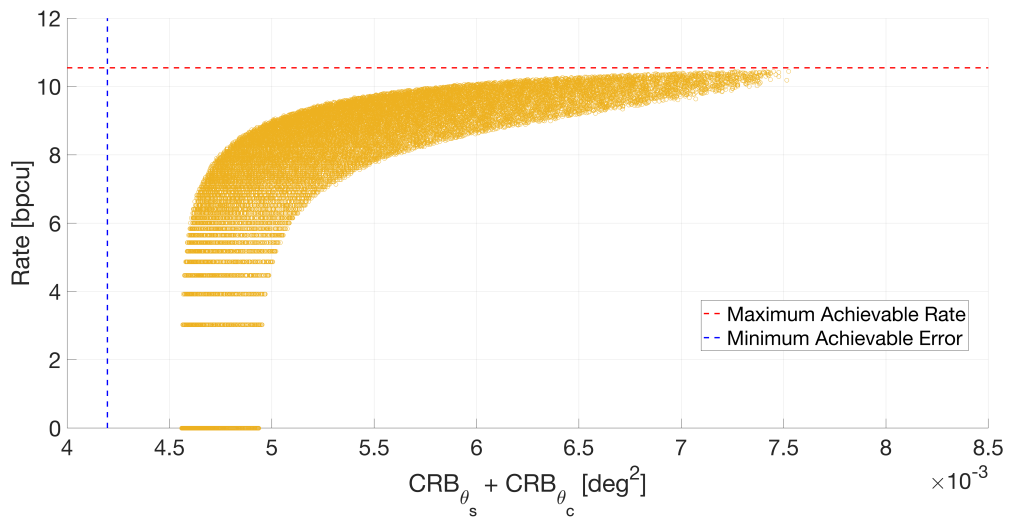


**Figure 6.15:** Third Strategy, First Direction Choice, Total BCRB-Rate Simulated Points.

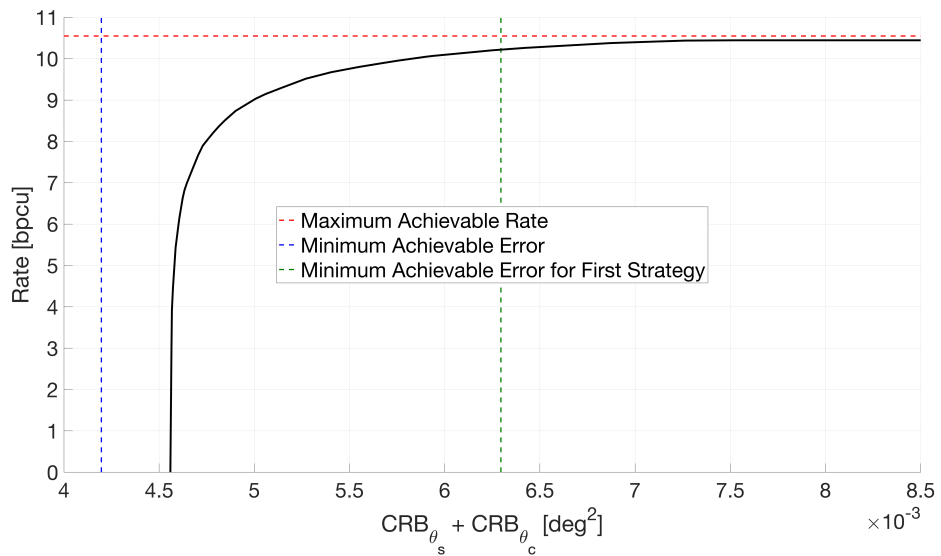


**Figure 6.16:** Third Strategy, First Direction Choice, Total BCRB-Rate Outer Bound.



This could provide a valid strategy for using ISAC in this two-angle scenario, using proper power allocation between the beams if we want to minimize the joint angle estimation error.

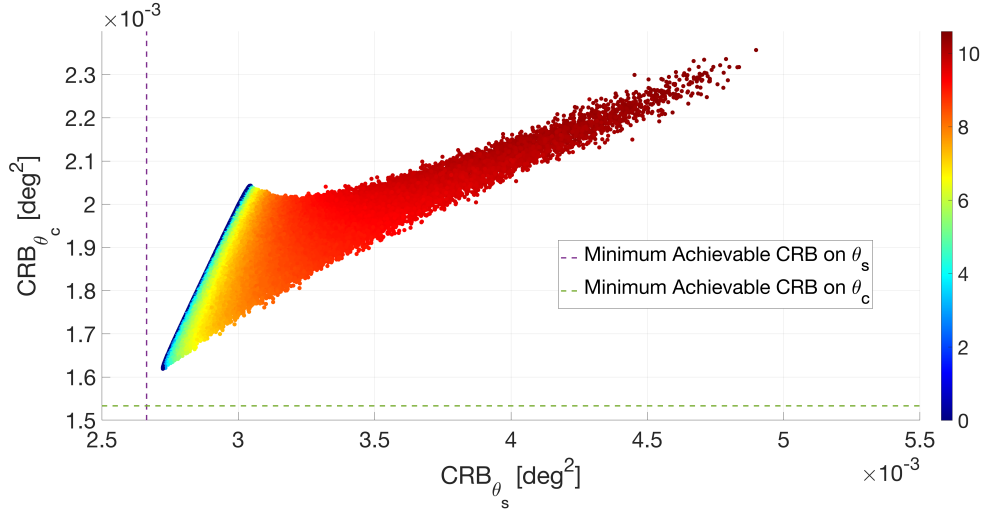


**Figure 6.17:** Third Strategy, Second Direction Choice, BCRB-Rate Simulated Points.

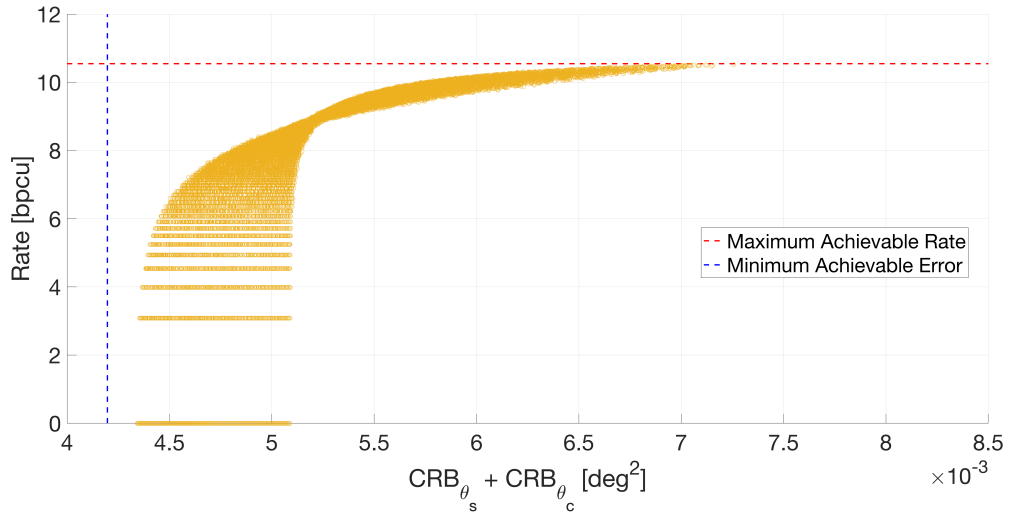


**Figure 6.18:** Third Strategy, Second Direction Choice, Total BCRB-Rate Simulated Points.

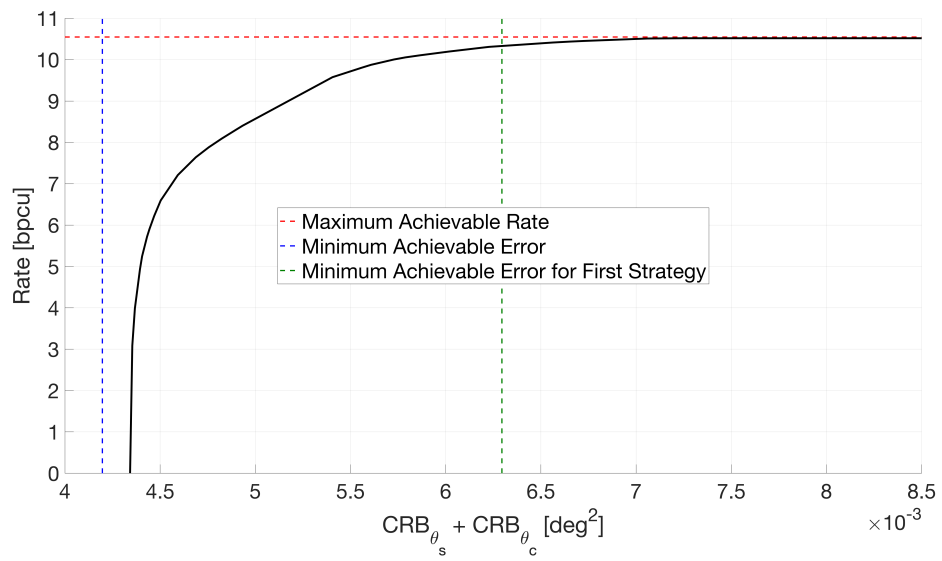


**Figure 6.19:** Third Strategy, Second Direction Choice, Total BCRB-Rate Outer Bound.

### 6.3.3 Choice 3: Spanning among the main eigenvector of $\bar{\mathbf{M}}_1$ , the main eigenvector of $\bar{\mathbf{M}}_2$ , the Directions of the Optimal Sensing, and the Direction of Optimal Communication

Finally, we combine the previous choices of directions seen in this strategy to obtain what we expect to be the more comprehensive inner bound for ISAC performance (in terms of BCRB-Rate tradeoff) in this scenario.

In 6.20, we can appreciate that the optimal points for single angle estimation and points focusing on the joint estimation are now reached.

It is key to compare in 6.23 the difference among the different direction choices while using this transmission strategy. These results provide a more comprehensive inner bound for the considered ISAC scenario.

Finally, it is possible to compare in 6.24 the overall comparison between the choices presented for the first strategy and those presented for the third one, further validating what has been discussed and commented on.

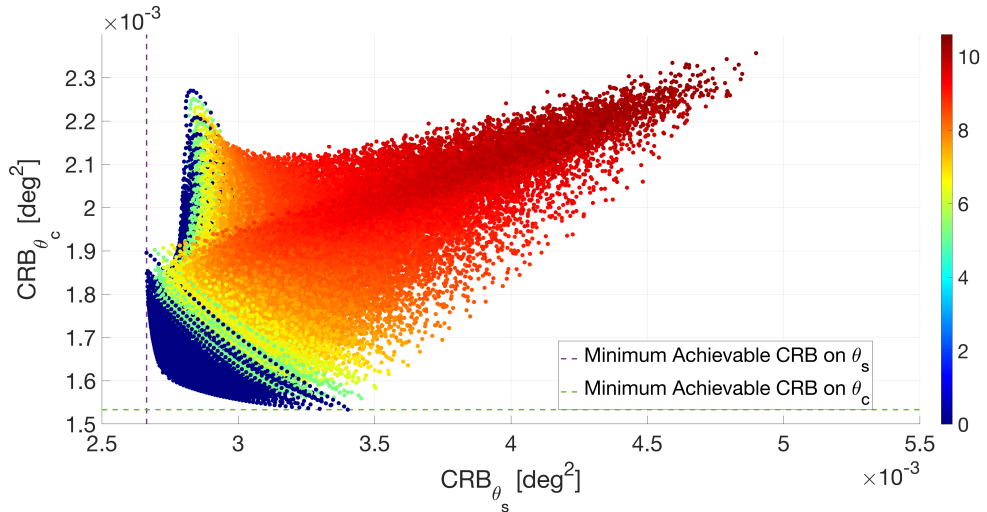


**Figure 6.20:** Third Strategy, Third Direction Choice, BCRB-Rate Simulated Points.

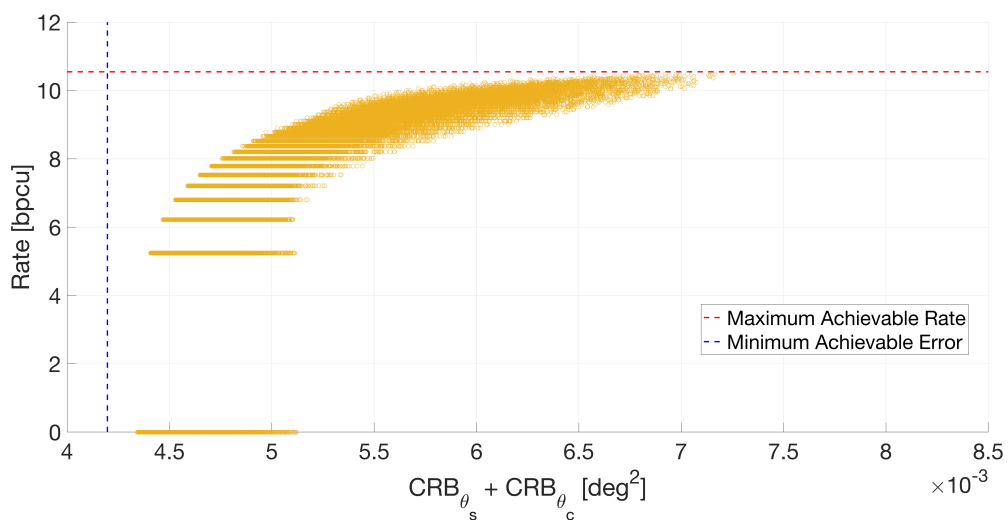


**Figure 6.21:** Third Strategy, Third Direction Choice, Total BCRB-Rate Simulated Points.

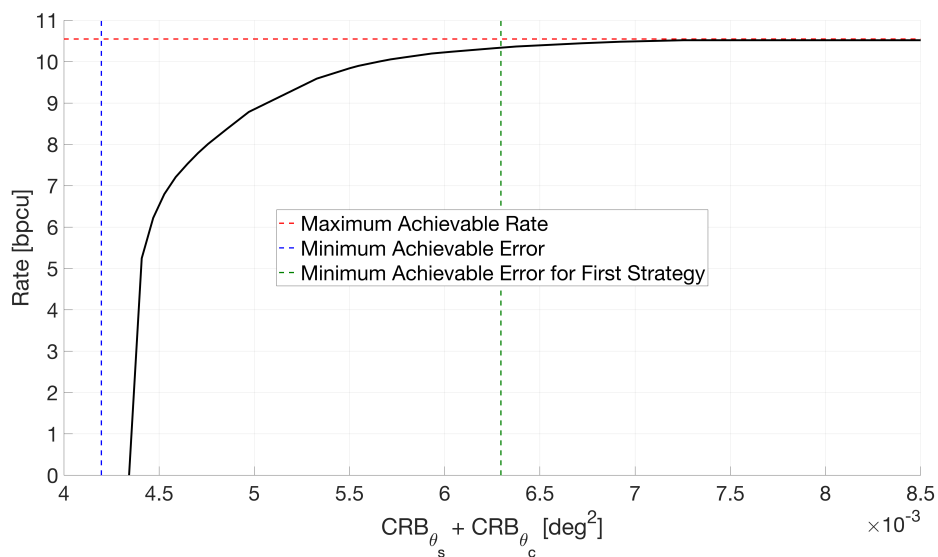


**Figure 6.22:** Third Strategy, Third Direction Choice, Total BCRB-Rate Outer Bound.

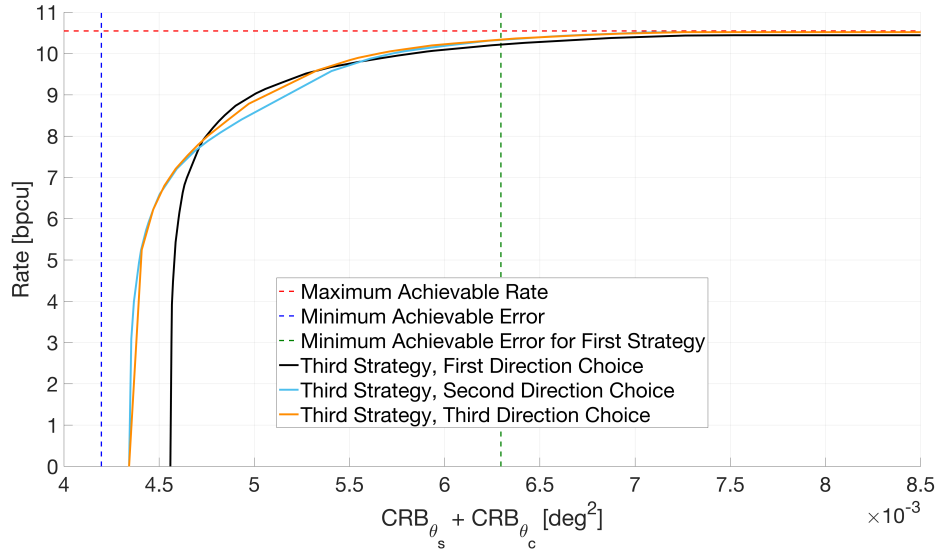


**Figure 6.23:** Third Strategy, Comparison of Direction Choice, Total BCRB-Rate Outer Bound.

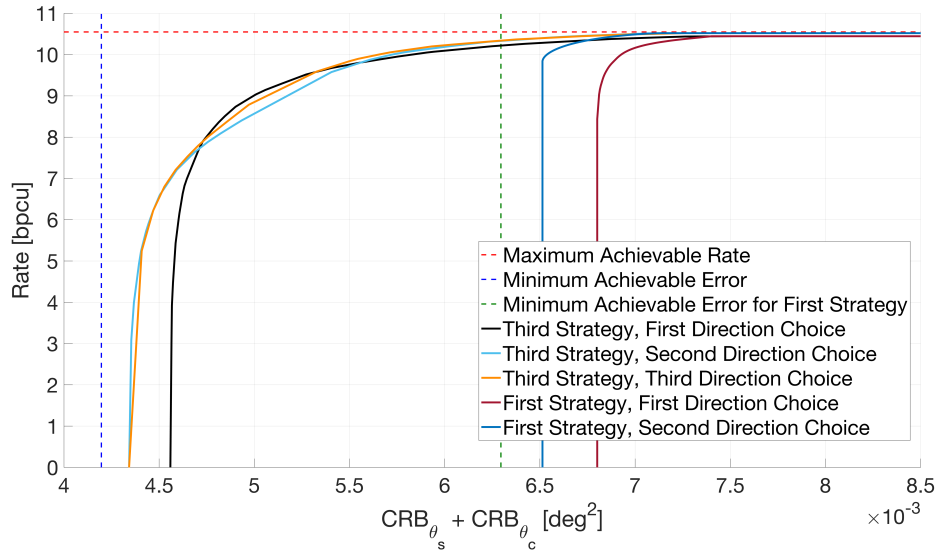


**Figure 6.24:** First and Third Strategy, Comparison of Direction Choice, Total BCRB-Rate Outer Bound.

# Chapter 7

## Conclusion

In this dissertation, we have conducted a comprehensive analysis of the ISAC tradeoff in a practical scenario involving the joint estimation of two targets, where one target is also an end-user for communication. This scenario represents a crucial step towards generalizing ISAC systems to more complex environments with multiple targets.

This work contributes by deriving the Bayesian Cramer-Rao Bound (BCRB) for the joint estimation of two angles of arrival representing the sensing and communication targets. Under certain assumptions, we demonstrated that the BCRB can be reduced to a sum of single-target estimation bounds, simplifying the analysis. Furthermore, we employed convex optimization techniques (CVX) to obtain the optimal sensing solution.

We have characterized the outer bound for the BCRB-Rate region, which describes the fundamental tradeoff between sensing accuracy and communication rate in ISAC systems. This was achieved by identifying the optimal sensing and communication points, providing valuable insights into the limits of ISAC performance.

We explored several achievable inner bounds through different transmission strategies to further understand and characterize these limits. These strategies involved one or two beams aimed at the sensing direction, communication direction, or a combination thereof. We identified a promising transmission strategy that allows achieving the optimal sensing and communication points based on the power allocation, effectively balancing the sensing and communication requirements.

This work represents a significant step forward in understanding and fully characterizing the ISAC tradeoff, a critical aspect of exploiting the full potential of this emerging technology. The theoretical foundations established in this dissertation pave the way for more efficient and effective integration of sensing and communication in future wireless networks, enabling a wide range of applications that demand seamless convergence of these functionalities.

Looking ahead, the insights and methodologies developed in this research can serve as a foundation for further exploration and generalization to more complex ISAC scenarios, ultimately driving the development of innovative solutions that push the boundaries of what is achievable in integrated sensing and communication systems.

# Appendix A

## Matlab Code

```
1 clc
2 close all
3 clear all
4 format longG
5
6 %% Simulation Parameters
7 theta_1 = deg2rad(30);      % Sensing target
8 theta_2 = deg2rad(42);      % Communication target
9 theta_1_var = deg2rad(5)^2;
10 theta_2_var = deg2rad(5)^2;
11
12 optimize_with_solver = false;
13 number_vectors_span_over = 4; % Remember to change granularity too
14 granularity = 1/40;          % Step size for discretization
15 transmission_strategy = 'third'; % Select 'first', 'second', or '
    third'
16
17 n_sim_theta_s = 1e4;
18 n_sim_theta_c = 1e2;
19 n_sim_gauss = 1e4;
20
21 N_T = 10;
22 k = 2*pi;
23 d_lambda = 0.5;
24 T = 3;
25 SNR_s = 20;          % maximum SNR of sensing RX in dB/antenna
26 SNR_c = 33;          % maximum SNR of communication RX in dB/
    antenna
27
28 save_figures = 0;
29 name_path = 'ResultsJune5'; % specify your path here
```



```

30 sim_type = '1_1_strategy'; % specify your simulation type string here
31
32 %% Plotting Parameters
33 FontAxis = 25;
34 FontSizenum = 25;
35 FontTitle = 25;
36 if isequal(transmission_strategy, 'first')
37     transmission_description = 'One Direction with Gaussian, e.g. \bf
38     X\rm = \surd{P_2}[\bf c\rm g_1,\bf c\rm g_2, ..., \bf c\rm g_T]';
39 elseif isequal(transmission_strategy, 'second')
40     transmission_description = 'One Direction without Gaussian, e.g.
41     \bf X\rm = \surd{P_1}[\bf s\rm,\bf s\rm, ..., \bf s\rm]';
42 elseif isequal(transmission_strategy, 'third')
43     transmission_description = 'One Direction with Gaussian and One
44     Without, e.g. \bf X\rm = [\surd{P_1}\bf s\rm + \surd{P_2}\bf c\rm
45     g_1, ..., \surd{P_1}\bf s\rm + \surd{P_2}\bf c\rm g_T]';
46 else
47     error('Incorrect Choice of Transmission Strategy')
48 end
49
50 num_fig = 0;
51 fig_names = {};
52
53 %% Precomputation of Useful Variables
54 rng(665093593) % Fixing seed
55 zero_tol = 1e-12; % To check computations with Matlab's
56 precision
57 N_T_vec = -(N_T-1)/2:(N_T-1)/2;
58 SNR_s_lin = db2pow(SNR_s);
59 SNR_c_lin = db2pow(SNR_c);
60
61 if isequal(transmission_strategy, 'second')
62     n_sim_theta_c = 1;
63     n_sim_gauss = 1;
64 end
65
66 %% Initialization of Angle's Distributions and Priors
67 k_VonMises_1 = double(find_k_VonMises(theta_1_var))*2;
68 theta_1_vec = circ_vmrnd(theta_1, k_VonMises_1, [1, n_sim_theta_s]);
69 I_0 = besseli(0,k_VonMises_1);
70 I_1 = besseli(1,k_VonMises_1);
71 J_theta_P_1 = (1-I_1^2/I_0^2)^(-1);
72
73 k_VonMises_2 = double(find_k_VonMises(theta_2_var))*2;
74 theta_2_vec = circ_vmrnd(theta_2, k_VonMises_2, [1, n_sim_theta_s]);
75 theta_c_vec = circ_vmrnd(theta_2, k_VonMises_2, [1, n_sim_theta_c]);
76 I_0 = besseli(0,k_VonMises_2);
77 I_1 = besseli(1,k_VonMises_2);
78 J_theta_P_2 = (1-I_1^2/I_0^2)^(-1);

```

```

74 |
75 | J_theta_P = [J_theta_P_1, 0;
76 |             0, J_theta_P_2];
77 |
78 | %% Communication Steering Vector
79 | h_c = zeros(N_T, n_sim_theta_c);
80 | for ind_theta_c = 1:n_sim_theta_c
81 |     h_c(:, ind_theta_c) = exp(1i * N_T_vec * k * d_lambda * cos(
82 |         theta_c_vec(ind_theta_c))).';    % rx steering vector (comm)
83 | end
84 | h_c_true = exp(1i * N_T_vec * k * d_lambda * cos(theta_2)).';
85 | h_c_true_hat = h_c_true/norm(h_c_true);
86 | max_rate_theo = find_Rate(1, h_c_true_hat, h_c, n_sim_theta_c,
87 |     SNR_c_lin);
88 | %% Sensing Steering Vectors
89 | M_1 = zeros(N_T, N_T, n_sim_theta_s);
90 | M_2 = zeros(N_T, N_T, n_sim_theta_s);
91 | for iter = 1:n_sim_theta_s
92 |     a_1 = exp(-1i * N_T_vec * k * d_lambda * cos(theta_1_vec(iter)))
93 |         .';    % tx steering vector
94 |     a_2 = exp(-1i * N_T_vec * k * d_lambda * cos(theta_2_vec(iter)))
95 |         .';    % rx steering vector (comm)
96 |     a_1_dot = a_1 .* (1i * N_T_vec * k * d_lambda * sin(theta_1_vec(
97 |         iter))).';
98 |     a_2_dot = a_2 .* (1i * N_T_vec * k * d_lambda * sin(theta_2_vec(
99 |         iter))).';
100 |
101 |     M_1(:, :, iter) = norm(a_1_dot)^2 * (a_1 * a_1') ...
102 |         + norm(a_1)^2 * (a_1_dot * a_1_dot');
103 |     M_2(:, :, iter) = norm(a_2_dot)^2 * (a_2 * a_2') ...
104 |         + norm(a_2)^2 * (a_2_dot * a_2_dot');
105 |
106 |     if n_sim_theta_s == 1
107 |         a_1 = exp(-1i * N_T_vec * k * d_lambda * cos(theta_1)).';
108 |         % tx steering vector
109 |         a_2 = exp(-1i * N_T_vec * k * d_lambda * cos(theta_2)).';
110 |         % rx steering vector (comm)
111 |         a_1_dot = a_1 .* (1i * N_T_vec * k * d_lambda * sin(theta_1))
112 |             .';
113 |         a_2_dot = a_2 .* (1i * N_T_vec * k * d_lambda * sin(theta_2))
114 |             .';
115 |
116 |         M_1 = norm(a_1_dot)^2 * (a_1 * a_1') ...
117 |             + norm(a_1)^2 * (a_1_dot * a_1_dot');
118 |         M_2 = norm(a_2_dot)^2 * (a_2 * a_2') ...
119 |             + norm(a_2)^2 * (a_2_dot * a_2_dot');
120 |     end

```

```

113 end
114
115 M_1_bar = mean(conj(M_1), 3);
116 M_2_bar = mean(conj(M_2), 3);
117
118 [V_M_1_bar, D_M_1_bar] = eig(M_1_bar);
119 [V_M_2_bar, D_M_2_bar] = eig(M_2_bar);
120
121 v_1_hat = V_M_1_bar(:, N_T-1);
122 v_2_hat = V_M_1_bar(:, N_T);
123
124 v_3_hat = V_M_2_bar(:, N_T-1);
125 v_4_hat = V_M_2_bar(:, N_T);
126
127 if optimize_with_solver
128     R_x_opt = R_x_opt_solver(N_T, T, SNR_s_lin, J_theta_P, M_1_bar,
129     M_2_bar);
129     [V_opt, D_opt] = eig(R_x_opt);
130     v_1_opt = V_opt(:, N_T);
131     v_2_opt = V_opt(:, N_T-1);
132 end
133
134 %% Finding theoretical boundaries
135 min_eps_1_theo = rad2deg(rad2deg(find_CRB_theo(v_2_hat, v_2_hat,
136     M_1_bar, J_theta_P(1,1), SNR_s_lin, T, N_T, 'second')));
137 min_eps_2_theo = rad2deg(rad2deg(find_CRB_theo(v_4_hat, v_4_hat,
138     M_2_bar, J_theta_P(2,2), SNR_s_lin, T, N_T, 'second')));
139 tot_min_eps_theo = min_eps_1_theo + min_eps_2_theo;
140
141 first_eps_1_theo = rad2deg(rad2deg(find_CRB_theo(v_2_hat, v_2_hat,
142     M_1_bar, J_theta_P(1,1), SNR_s_lin, T, N_T, 'first')));
143 first_eps_2_theo = rad2deg(rad2deg(find_CRB_theo(v_4_hat, v_4_hat,
144     M_2_bar, J_theta_P(2,2), SNR_s_lin, T, N_T, 'first')));
145 tot_first_eps_theo = first_eps_1_theo + first_eps_2_theo;
146
147 %% Simulation
148 Lambdas = generateCombinations(number_vectors_span_over, granularity)
149 ;
150 [row_Lambdas, ~] = size(Lambdas);
151 eps_1_theo = zeros(1, row_Lambdas);
152 eps_2_theo = zeros(1, row_Lambdas);
153 eps_1_avg_gauss = zeros(1, row_Lambdas);
154 eps_2_avg_gauss = zeros(1, row_Lambdas);
155 rate = zeros(1, row_Lambdas);
156
157 for ind_1 = 1:row_Lambdas
158     lambda = Lambdas(ind_1,:);
159
160     r_1_tx = zeros(N_T,1);

```

```

156   r_2_tx = zeros(N_T,1) + sqrt(lambda(1)) * v_1_hat + sqrt(lambda
(2)) * v_2_hat + sqrt(lambda(3)) * v_3_hat + sqrt(lambda(4)) *
v_4_hat;
157   p_1_tx = 0;
158   p_2_tx = lambda(1) + lambda(2) + lambda(3) + lambda(4);
159
160   if isequal(transmission_strategy, 'first') && p_1_tx~=0
161       error('Inconsistent choice of power with transmission
strategy. With first strategy p_1_tx should always be 0.')
162   elseif isequal(transmission_strategy, 'second') && p_2_tx~=0
163       error('Inconsistent choice of power with transmission
strategy. With second strategy p_2_tx should always be 0.')
164   end
165
166   r_1_tx_hat = normalized(r_1_tx);
167   r_2_tx_hat = normalized(r_2_tx);
168   if isnan(r_1_tx_hat)
169       r_1_tx_hat = zeros(N_T, 1);
170   elseif isnan(r_2_tx_hat)
171       r_2_tx_hat = zeros(N_T,1);
172   end
173
174   [err_1_theo, err_2_theo, err_1_avg_gauss, err_2_avg_gauss,
rate_out] = myfun(p_1_tx, p_2_tx, r_1_tx_hat, r_2_tx_hat,...
175               M_1_bar, M_2_bar, T, N_T, SNR_s_lin, J_theta_P,
n_sim_gauss, h_c, n_sim_theta_c, SNR_c_lin, transmission_strategy)
;
176
177   eps_1_theo(ind_1) = err_1_theo;
178   eps_2_theo(ind_1) = err_2_theo;
179   eps_1_avg_gauss(ind_1) = err_1_avg_gauss;
180   eps_2_avg_gauss(ind_1) = err_2_avg_gauss;
181   rate(ind_1) = rate_out;
182 end
183
184 %% Finding minimum error and maximum rate points
185 tot_eps_gauss = eps_1_avg_gauss + eps_2_avg_gauss;
186 vec_eps_theo_2D = linspace(min(tot_eps_theo), max(tot_eps_theo), 2);
187 vec_eps_1_theo_3D = linspace(min(eps_1_theo), max(eps_1_theo), 2);
188 vec_eps_2_theo_3D = linspace(min(eps_2_theo), max(eps_2_theo), 2);
189 vec_eps_gauss_2D = linspace(min(tot_eps_gauss), max(tot_eps_gauss),
2);
190 vec_eps_1_gauss_3D = linspace(min(eps_1_avg_gauss), max(
eps_1_avg_gauss), 2);
191 vec_eps_2_gauss_3D = linspace(min(eps_2_avg_gauss), max(
eps_2_avg_gauss), 2);
192 vec_rate = linspace(min(rate), max(rate), 2);
193
194 %% Plotting 2D Thoretical

```

```

195 if isequal(transmission_strategy, 'first')
196     num_fig = num_fig + 1;
197     fig_names{end + 1} = 'BCRB_tot-Rate_Theo';
198     figure
199     hold on
200     plot(vec_eps_theo_2D, max_rate_theo*ones(1,2), 'r—', LineWidth
=2)
201     plot(tot_min_eps_theo*ones(1,2), vec_rate, 'b—', LineWidth=2)
202     scatter(eps_1_theo + eps_2_theo, rate)
203     grid on
204     set(gca, 'FontSize', FontAxis);
205     title(['Total BCRB-Rate Theoretical Points for \theta_s = ',
num2str(round(rad2deg(theta_1))) ,...
206         '\theta_o and \theta_c = ', num2str(round(rad2deg(theta_2))), '
^o, T = ', num2str(T)], 'FontSize', FontTitle)
207     subtitle(['Transmission Strategy: ', transmission_description], '
FontSize', FontTitle-2)
208
209     xlabel('CRB_{\theta_1} + CRB_{\theta_2} [deg^2]', 'FontSize',
FontSizenum)
210     ylabel('Rate [bpcu]', 'FontSize', FontSizenum)
211 end
212 %% Plotting 2D Gaussian
213 if ~isequal(transmission_strategy, 'second')
214     num_fig = num_fig + 1;
215     fig_names{end + 1} = 'BCRB_tot-Rate_Gauss';
216     figure
217     hold on
218     plot([tot_min_eps_theo-0.001, tot_min_eps_theo+0.01],
max_rate_theo*ones(1,2), 'r—', LineWidth=2)
219     plot(tot_min_eps_theo*ones(1,2), [-1,max_rate_theo+5], 'b—',
LineWidth=2)
220     scatter(eps_1_avg_gauss + eps_2_avg_gauss, rate)
221     grid on
222     legend('Maximum Achievable Rate', 'Minimum Achievable Error', '
Location', 'best')
223     set(gca, 'FontSize', FontAxis);
224     title(['Total BCRB-Rate Simulated Points for \theta_s = ',
num2str(round(rad2deg(theta_1))) ,...
225         '\theta_o and \theta_c = ', num2str(round(rad2deg(theta_2))), '
^o, T = ', num2str(T)], 'FontSize', FontTitle)
226     subtitle(['Transmission Strategy: ', transmission_description], '
FontSize', FontTitle-2)
227
228     xlabel('CRB_{\theta_1} + CRB_{\theta_2} [deg^2]', 'FontSize',
FontSizenum)
229     ylabel('Rate [bpcu]', 'FontSize', FontSizenum)
230     xlim([4, 8.5]*1e-3)
231     ylim([0,12])

```

```

232 end
233 %% Plotting 3D Theoretical with Colors
234 if ~isequal(transmission_strategy, 'third')
235     num_fig = num_fig + 1;
236     fig_names{end + 1} = 'BCRB-Rate_Theo';
237     figure
238     hold on
239     plot(vec_eps_1_theo_3D, min_eps_2_theo*ones(1,2), '—', 'color',
240          [0.1, 0.1, 0.1], LineWidth=2)
241     plot(min_eps_1_theo*ones(1,2), vec_eps_2_theo_3D, '—', 'color',
242          [0.5, 0.5, 0.5], LineWidth=2)
243     scatter(eps_1_theo, eps_2_theo, [], rate, 'filled')
244     colormap(jet)
245     colorbar
246     grid on
247     set(gca, 'FontSize', FontAxis);
248     title(['BCRB-Rate Theoretical Points for \theta_s = ', num2str(
249           round(rad2deg(theta_1))) ,...
250           '\theta_c = ', num2str(round(rad2deg(theta_2))), '\theta_o, T = ',
251           num2str(T)], 'FontSize', FontTitle)
252     subtitle(['Transmission Strategy: ', transmission_description], '
253             FontSize', FontTitle-2)
254
255     xlabel('CRB_{\theta_1} [deg^2]', 'FontSize', FontSizenum)
256     ylabel('CRB_{\theta_2} [deg^2]', 'FontSize', FontSizenum)
257     zlabel('Rate [bpcu]', 'FontSize', FontSizenum)
258 end
259 %% Plotting 3D Gaussian with Colors
260 num_fig = num_fig + 1;
261 fig_names{end + 1} = 'BCRB-Rate_Gauss';
262 figure
263 hold on
264 plot(vec_eps_1_gauss_3D, min_eps_2_theo*ones(1,2), '—', 'color',
265      [0.1, 0.1, 0.1], LineWidth=2)
266 plot(min_eps_1_theo*ones(1,2), vec_eps_2_gauss_3D, '—', 'color',
267      [0.5, 0.5, 0.5], LineWidth=2)
268 scatter(eps_1_avg_gauss, eps_2_avg_gauss, [], rate, 'filled')
269 colormap(jet)
270 colorbar
271 grid on
272 set(gca, 'FontSize', FontAxis);
273 title(['BCRB-Rate Simulated Points for \theta_s = ', num2str(round(
274       rad2deg(theta_1))) ,...
275       '\theta_c = ', num2str(round(rad2deg(theta_2))), '\theta_o,
276       T = ', num2str(T)], 'FontSize', FontTitle)
277 subtitle(['Transmission Strategy: ', transmission_description], '
278         FontSize', FontTitle-2)
279 % caxis([6.2, 10.8])
280 % xlim([min(eps_1_theo)-0.3 * 1e-3, max(eps_1_theo)+0.3 * 1e-3])

```

```

271 % ylim([min(eps_2_theo)-0.3 * 1e-3, max(eps_2_theo)+0.3 * 1e-3])
272
273 xlabel('CRB_{\theta_1} [deg^2]', 'FontSize', FontSizenum)
274 ylabel('CRB_{\theta_2} [deg^2]', 'FontSize', FontSizenum)
275 zlabel('Rate [bpcu]', 'FontSize', FontSizenum)
276
277 %% Plotting Outer Bound
278 if ~isequal(transmission_strategy, 'second')
279     if isequal(transmission_strategy, 'first')
280         x = tot_eps_theo;
281     else
282         x = tot_eps_gauss;
283     end
284     y = rate;
285
286     % Combine x and y into a matrix of points
287     points = [x(:), y(:)];
288     % Compute the convex hull
289     hullIndices = convhull(points(:,1), points(:,2));
290     % Extract the hull points
291     hullPoints = points(hullIndices, :);
292     % Get the left and top side points
293     boundaryPoints = getLeftTopSidePoints(hullPoints);
294
295     figure
296     num_fig = num_fig + 1;
297     fig_names{end + 1} = 'Outer_Bound';
298     hold on
299     plot([tot_min_eps_theo-0.01, tot_min_eps_theo+0.01],
300          max_rate_theo*ones(1,2), 'r—', LineWidth=2)
301     plot(tot_min_eps_theo*ones(1,2), [-1,max_rate_theo+5], 'b—',
302          LineWidth=2)
303     plot(boundaryPoints(:,1), boundaryPoints(:,2), 'k-', LineWidth=3)
304     grid on
305     legend('Maximum Achievable Rate', 'Minimum Achievable Error', '
306           Location', 'best')
307     set(gca, 'FontSize', FontAxis);
308     title(['Total BCRB-Rate Simulated Bound for \theta_s = ', num2str
309           (round(rad2deg(theta_1))) , ...
310           '\theta_c = ', num2str(round(rad2deg(theta_2))), '
311           ^o, T = ', num2str(T)], 'FontSize', FontTitle)
312     subtitle(['Transmission Strategy: ', transmission_description], '
313             FontSize', FontTitle-2)
314
315     xlabel('CRB_{\theta_1} + CRB_{\theta_2} [deg^2]', 'FontSize',
316            FontSizenum)
317     ylabel('Rate [bpcu]', 'FontSize', FontSizenum)
318     xlim([4, 8.5]*1e-3)
319     ylim([0, 12])

```

```

313 end
314 %% Save figures
315 if save_figures
316     % Loop over each figure
317     for i = 1:num_fig
318         % Create a figure if it doesn't exist (comment this line if
319         figures already exist)
320         figure(i); % this line is just to create sample figures
321
322         % Resize the figure to full screen or a specific size
323         set(gcf, 'Units', 'normalized', 'OuterPosition', [0 0 1 1]);
324
325         % Generate the full path for the figure
326         file_name = strcat(name_path, '/', fig_names{i}, '/',
327         sim_type);
328
329         savefig(gcf, [file_name '.fig'])
330         print(gcf, file_name, ['-d', 'png'], '-r300');
331
332     end
333 end
334 %% Functions
335 function [err_1_theo, err_2_theo, err_1_avg_gauss, err_2_avg_gauss,
336         rate_out] = myfun(p_1_tx, p_2_tx, r_1_tx, r_2_tx, ...
337         M_1_bar, M_2_bar, T, N_T, SNR_s_lin, J_theta_P,
338         n_sim_gauss, h_c, n_sim_theta_c, SNR_c_lin, option_theo)
339
340     [err_1_theo] = find_CRB_theo(r_1_tx, r_2_tx, M_1_bar, J_theta_P
341     (1,1), SNR_s_lin, T, N_T, option_theo);
342     [err_2_theo] = find_CRB_theo(r_1_tx, r_2_tx, M_2_bar, J_theta_P
343     (2,2), SNR_s_lin, T, N_T, option_theo);
344
345     [err_1_avg_gauss] = find_CRB_avg(p_1_tx, p_2_tx, r_1_tx, r_2_tx,
346     M_1_bar, J_theta_P(1,1), SNR_s_lin, T, N_T, n_sim_gauss);
347     [err_2_avg_gauss] = find_CRB_avg(p_1_tx, p_2_tx, r_1_tx, r_2_tx,
348     M_2_bar, J_theta_P(2,2), SNR_s_lin, T, N_T, n_sim_gauss);
349
350     rate_out = find_Rate(p_2_tx, r_2_tx, h_c, n_sim_theta_c,
351     SNR_c_lin);
352
353     err_1_theo = rad2deg(rad2deg(err_1_theo));
354     err_2_theo = rad2deg(rad2deg(err_2_theo));
355
356     err_1_avg_gauss = rad2deg(rad2deg(err_1_avg_gauss));
357     err_2_avg_gauss = rad2deg(rad2deg(err_2_avg_gauss));
358 end

```



```

352 function [err_theo] = find_CRB_theo(r_1_tx, r_2_tx, M_bar, J_theta,
SNR_s_lin, T, N_T, option_theo)
353     if isequal(option_theo, 'first')
354         R_x = r_2_tx * r_2_tx';
355         corr_term = 0;
356         psi = real(J_theta * (2*SNR_s_lin*trace(M_bar*R_x))^(−1));
357         if T==1
358             err_theo = real( (SNR_s_lin * trace(M_bar * R_x))^(−1) *
psi^(T−1) * exp(psi) * gammainc(psi, 1−T) );
359         else
360             for n=1:T−2
361                 prod_denom = 1;
362                 for i=1:n
363                     prod_denom = prod_denom * (T−i−1);
364                 end
365                 new_term = ((−1)^n * psi^n) / (prod_denom) + (−1)^(T
−1)* (exp(psi)*psi^(T−1)*gammainc(psi, 0)) / (gamma(T−1));
366                 corr_term = corr_term + new_term;
367             end
368             err_theo = real(( 2 * (T−1) * SNR_s_lin * trace(M_bar *
R_x))^(−1) * (1+corr_term));
369         end
370         elseif isequal(option_theo, 'second')
371             R_x = r_1_tx * r_1_tx';
372             err_theo = real((2 * T * SNR_s_lin * trace(M_bar * R_x) +
J_theta)^(−1));
373         elseif isequal(option_theo, 'third')
374             R_x = r_1_tx * r_1_tx';
375             err_theo = real((2 * T * SNR_s_lin * trace(M_bar * R_x) +
J_theta)^(−1));
376         end
377     end
378
379 function [err_gauss_avg] = find_CRB_avg(p_1_tx, p_2_tx, r_1_tx,
r_2_tx, M_bar, J_theta, SNR_s_lin, T, N_T, n_sim_gauss)
380     err_gauss = zeros(1, n_sim_gauss);
381     gauss_rnd = (1/sqrt(2)) * (randn(T, n_sim_gauss) + 1i * randn(T,
n_sim_gauss));
382     for ind_gauss = 1:n_sim_gauss
383         X_tx = zeros(N_T, T);
384         for t=1:T
385             X_tx(:, t) = sqrt(p_1_tx)*r_1_tx + sqrt(p_2_tx)*r_2_tx *
gauss_rnd(t, ind_gauss);
386         end
387         R_x_gauss = 1/T * (X_tx * X_tx');
388
389         err_gauss(ind_gauss) = real((2 * T * SNR_s_lin * trace(M_bar
* R_x_gauss) + J_theta)^(−1));
390

```

```

391     end
392     err_gauss_avg = mean(err_gauss);
393 end
394
395 function rate_avg = find_Rate(p_2_tx, r_2_tx, h_c, n_sim_theta_c,
    SNR_c_lin)
396     rate = zeros(1, n_sim_theta_c);
397     R_x = r_2_tx * r_2_tx';
398     if p_2_tx == 0
399         rate_avg = 0;
400     else
401         for ind_theta_c = 1:n_sim_theta_c
402             rate(ind_theta_c) = log2(det(1 + norm(h_c(:,ind_theta_c))
    ^(-2) * real(h_c(:,ind_theta_c))' * R_x * h_c(:,ind_theta_c)) *
    SNR_c_lin * p_2_tx));
403         end
404         rate_avg = mean(rate);
405     end
406 end
407
408 function [R_x_opt] = R_x_opt_solver(N_T, T, SNR_s_lin, J_theta_P,
    M_1_bar, M_2_bar)
409     % Initialize CVX
410     cvx_begin sdp
411         % Variable definition
412         variable X(N_T, N_T) hermitian
413         variable eps_1
414         variable eps_2
415         variable t1
416         variable t2
417         minimize ( eps_1 + eps_2 )
418
419         % Constraints
420         subject to
421             trace(X) == 1
422             X >= 0 % X must be positive semidefinite
423             2 * T * SNR_s_lin * trace(M_1_bar * X) + J_theta_P(1,1)
    >= t1
424             2 * T * SNR_s_lin * trace(M_2_bar * X) + J_theta_P(2,2)
    >= t2
425             eps_1 >= inv_pos(t1)
426             eps_2 >= inv_pos(t2)
427         cvx_end
428
429         % Optimal solution
430         R_x_opt = X;
431     end
432
433     % Function to find the left and top side points

```

```
434 function boundaryPoints = getLeftTopSidePoints(hullPoints)
435     % Sort the points by x-coordinate (ascending)
436     sortedPoints = sortrows(hullPoints, 2);
437     x = sortedPoints(:,1);
438     y = sortedPoints(:,2);
439
440     [min_x, ind_min_x] = min(x);
441     [max_y, ind_max_y] = max(y);
442     max_x = x(ind_max_y);
443     min_y = y(ind_min_x);
444
445     boundaryPoints = [];
446     maxsize = size(sortedPoints, 1);
447
448     % Loop through sorted points to find leftmost points
449     for i = 1:maxsize
450         if sortedPoints(i,1) >= min_x && sortedPoints(i,1) <= max_x
451             && sortedPoints(i,2) >= min_y && sortedPoints(i,2) <= max_y
452                 if i>1
453                     if sortedPoints(i,2) == boundaryPoints(end,2)
454                         else
455                             boundaryPoints = [boundaryPoints; sortedPoints(i,
456 1), sortedPoints(i, 2)];
457                         end
458                     else
459                         boundaryPoints = [boundaryPoints; sortedPoints(i, 1),
460 sortedPoints(i, 2)];
461                     end
462                 end
463             end
464         end
465
466         % if min(y)~=0
467         %     boundaryPoints = [min_x, 0; boundaryPoints];
468         % end
469         % if max_x < 8.5*1e-3
470         %     boundaryPoints = [boundaryPoints; 8.5*1e-3, max_y];
471         % end
472     end
473
474 function y = normalized(x)
475     y = x/norm(x);
476 end
```

# Bibliography

- [1] Yifeng Xiong, Fan Liu, Yuanhao Cui, Weijie Yuan, Tony Xiao Han, and Giuseppe Caire. «On the Fundamental Tradeoff of Integrated Sensing and Communications Under Gaussian Channels». In: *IEEE Transactions on Information Theory* 69.9 (Sept. 2023), pp. 5723–5751. DOI: 10.1109/TIT.2023.3284449 (cit. on pp. 1, 4, 6, 10, 14, 16, 20–22).
- [2] Harald Cramér. *Mathematical Methods of Statistics*. Princeton, NJ: Princeton University Press, 1946. ISBN: 0-691-08004-6 (cit. on p. 2).
- [3] Harry L. Van Trees. *Detection, Estimation, and Modulation Theory, Part I: Detection, Estimation, and Linear Modulation Theory*. 2nd. Hoboken, NJ, USA: Wiley, 2004, p. 716. ISBN: 978-0-471-46382-5 (cit. on p. 2).
- [4] Abbas El Gamal and Young-Han Kim. *Network Information Theory*. Cambridge, UK: Cambridge University Press, 2011. ISBN: 978-0521761451 (cit. on p. 3).
- [5] Milton Abramowitz and Irene A. Stegun, eds. *Handbook of Mathematical Functions*. Reprinted by Dover Publications, 1965. National Bureau of Standards, 1964. ISBN: 0-486-61272-4 (cit. on p. 3).
- [6] Yuanwei Liu, Zhaolin Wang, Jiaqi Xu, Chongjun Ouyang, Xidong Mu, and Robert Schober. «Near-Field Communications: A Tutorial Review». In: *IEEE Open Journal of the Communications Society* 4 (2023), pp. 1999–2049. DOI: 10.1109/OJCOMS.2023.3305583 (cit. on p. 3).
- [7] An Liu et al. «A Survey on Fundamental Limits of Integrated Sensing and Communication». In: *IEEE Communications Surveys & Tutorials* 24.2 (2022), pp. 994–1034. DOI: 10.1109/COMST.2022.3149272 (cit. on pp. 5, 6).
- [8] Dongning Guo, S. Shamai, and S. Verdu. «Mutual information and minimum mean-square error in Gaussian channels». In: *IEEE Transactions on Information Theory* 51.4 (2005), pp. 1261–1282. DOI: 10.1109/TIT.2005.844072 (cit. on p. 5).

- [9] Fan Liu, Yuanhao Cui, Christos Masouros, Jie Xu, Tony Xiao Han, Yonina C. Eldar, and Stefano Buzzi. «Integrated Sensing and Communications: Toward Dual-Functional Wireless Networks for 6G and Beyond». In: *IEEE Journal on Selected Areas in Communications* 40.6 (2022), pp. 1728–1767. DOI: 10.1109/JSAC.2022.3156632 (cit. on p. 5).
- [10] Yuanhao Cui, Fan Liu, Xiaojun Jing, and Junsheng Mu. «Integrating Sensing and Communications for Ubiquitous IoT: Applications, Trends, and Challenges». In: *IEEE Network* 35.5 (2021), pp. 158–167. DOI: 10.1109/MNET.010.2100152 (cit. on pp. 5, 6).
- [11] Weijie Yuan, Fan Liu, Christos Masouros, Jinhong Yuan, Derrick Wing Kwan Ng, and Nuria González-Prelcic. «Bayesian Predictive Beamforming for Vehicular Networks: A Low-Overhead Joint Radar-Communication Approach». In: *IEEE Transactions on Wireless Communications* 20.3 (2021), pp. 1442–1456. DOI: 10.1109/TWC.2020.3033776 (cit. on p. 5).
- [12] Yuan Shen, Henk Wymeersch, and Moe Z. Win. «Fundamental Limits of Wideband Localization— Part II: Cooperative Networks». In: *IEEE Transactions on Information Theory* 56.10 (2010), pp. 4981–5000. DOI: 10.1109/TIT.2010.2059720 (cit. on pp. 10, 14).
- [13] Jian Li, Luzhou Xu, Petre Stoica, Keith W. Forsythe, and Daniel W. Bliss. «Range Compression and Waveform Optimization for MIMO Radar: A Cramér–Rao Bound Based Study». In: *IEEE Transactions on Signal Processing* 56.1 (2008), pp. 218–232. DOI: 10.1109/TSP.2007.901653 (cit. on p. 12).
- [14] Michael Grant and Stephen Boyd. *CVX: Matlab Software for Disciplined Convex Programming, version 2.1*. <https://cvxr.com/cvx>. Mar. 2014 (cit. on p. 16).
- [15] Michael Grant and Stephen Boyd. «Graph implementations for nonsmooth convex programs». In: *Recent Advances in Learning and Control*. Ed. by V. Blondel, S. Boyd, and H. Kimura. Lecture Notes in Control and Information Sciences. [http://stanford.edu/~boyd/graph\\_dcp.html](http://stanford.edu/~boyd/graph_dcp.html). Springer-Verlag Limited, 2008, pp. 95–110 (cit. on p. 16).